CHAPTER 3

THE LANAWAY FIELD CASE STUDY

On the basis of conventional surface seismic data, an exploratory well (referred to as the VSP well in this chapter) was drilled in 1986 into the up-dip, raised rim of the Devonian Leduc Formation reef complex at Lanaway Field, southwestern Alberta, Canada. The stratigraphy of the Central Plains of the Western Canadian Sedimentary Basin is listed in Figures 3.1A, B, and C (representing the stratigraphic sequence from the Quaternary to the Cambrian Periods) .

The VSP well was expected to encounter an anomalous late-stage carbonate accretionary buildup at the Leduc level. It was anticipated that the Leduc at the VSP well location would be up to 80 m higher than at adjacent rim well sites. The envisioned accretionary growth was not present; the top of the Leduc in the VSP well was consistent with other rim wells along the Lanaway/Garrington reef trend (Fig. 3.2) and inconsistent with the seismic interpretation (Hinds et al., 1989a, Hinds et al., 1994a and 1994c). Fortunately, however, the Leduc was structurally closed and the VSP well was completed as an oil well (producing both from the Nisku and Leduc Formations).

In order to resolve the apparent discrepancy between the interpreted surface seismic data and geology at the VSP well, a near offset vertical seismic profile (VSP) was conducted at the

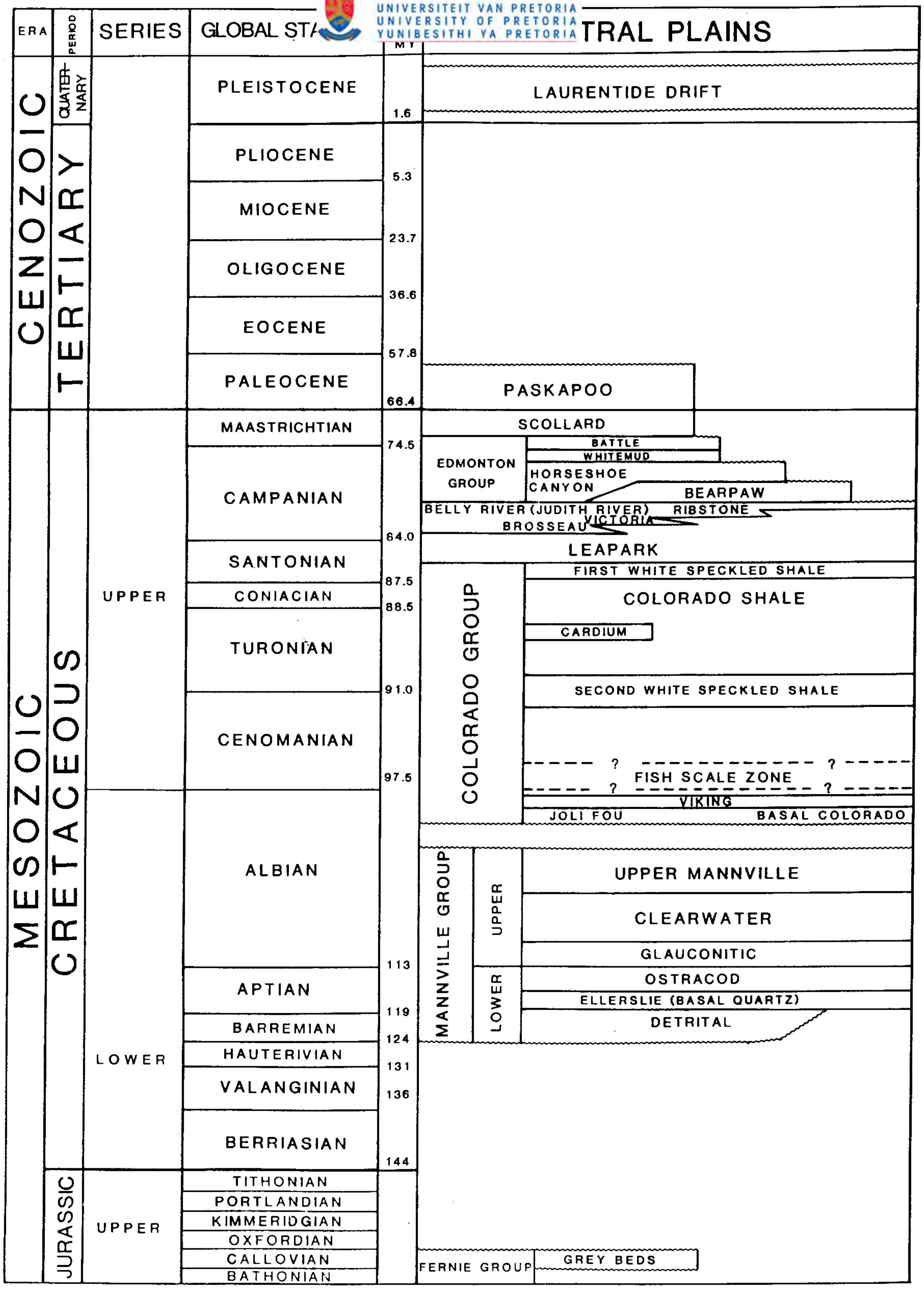

Figure 3.1A Stratigraphy from the Quaternary (Cenozoic) to the Upper Jurassic (Mesozoic) periods of the Central Plains area of the Western Canada Sedimentary Basin (after AGAT Laboratories, 1988; Anderson et al., 1989d; Hinds et al., 1994a and c)

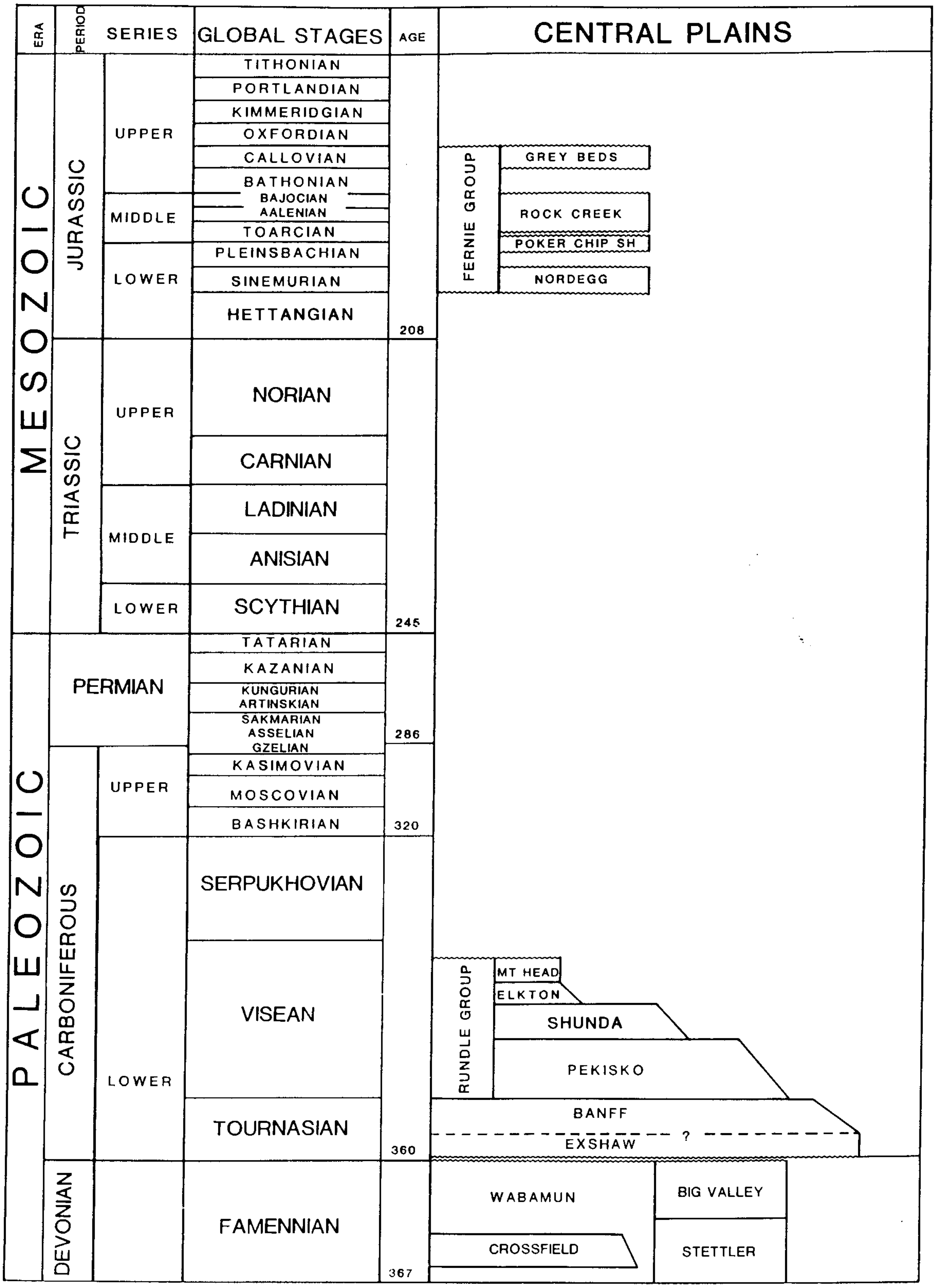

Figure 3.1B Stratigraphy from the Upper Jurassic (Mesozoic) to the Upper Devonian (Paleozoic) periods of the Central Plains area of the Western Canada Sedimentary Basin (after AGAT Laboratories, 1988; Anderson et al., 1989d; Hinds et al., 1994a and c)

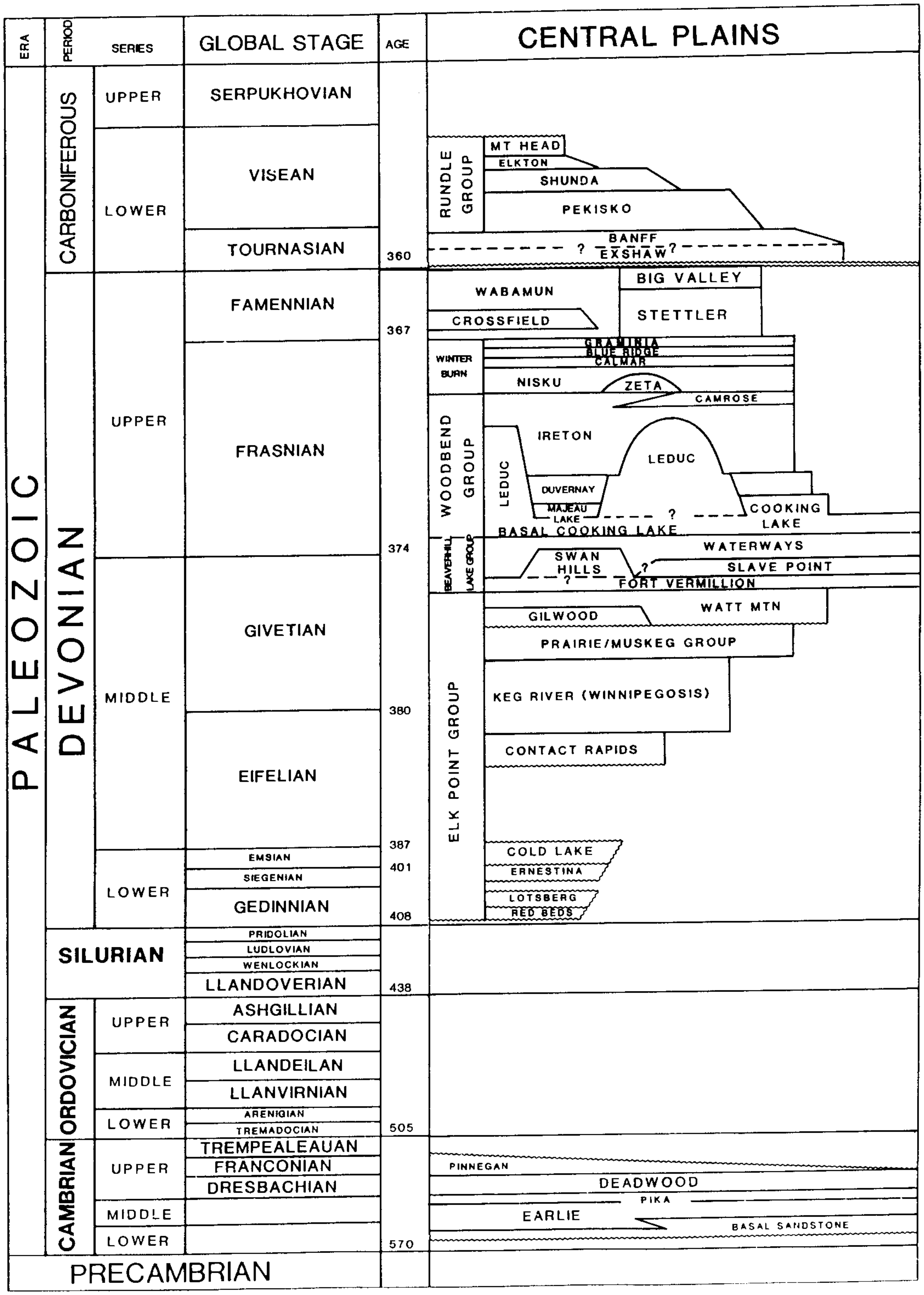

Figure 3.1C Stratigraphy from the Upper Carboniferous (Paleozoic) period to the Precambrian of the Central Plains area of Western Canada Sedimentary Basin (after AGAT Laboratories, 1988; Anderson et al., 1989d; and Hinds et al., 1994a and c)

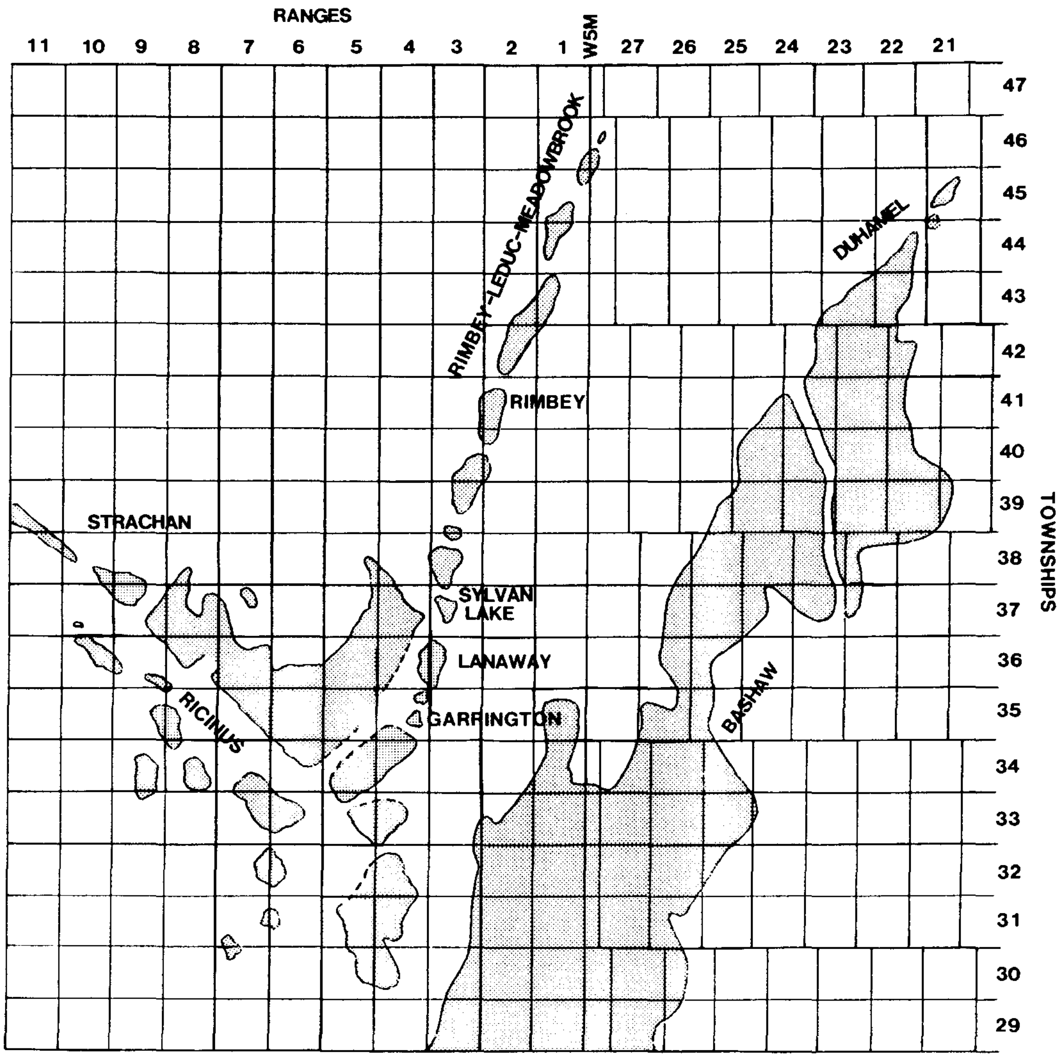

Figure 3.2 Regional location map of the Lanaway study area. The shaded areas represent the areal extent of the major Leduc Formation carbonate reefs of the area (with permission of Talisman Resources Inc.; from Hinds et al., 1994a and c)

well site. The interpretation of the VSP was expected to elucidate the geological origin of the misinterpreted seismic anomaly. Towards this end, the interpretation of the VSP was relatively successful in being able to assist in the formulation of an explanation for the anomaly. These data confirmed that the original interpretation of the surface seismic data (with respect to the Nisku, Ireton and Leduc top) was incorrect, and that the anomaly observed on the surface seismic line was not a processing artifact. The anomaly could most probably be attributed to either 1) structural relief at the pre-Cretaceous subcrop (as exemplified by Shunda Formation isopach values); 2) stratigraphic anomalies (thicker sections of carbonates) within the Winterburn Group or 3) seismic focusing caused by draping Ireton over the nose of the reef along the traverse of the seismic line. Interbed multiples interfering with the Nisku event could possibly be a minor contributing factor.

3.1 Carbonate reef development in the Western Canadian Sedimentary Basin

As an introduction to the geology of the carbonate reef case studies presented in this chapter (Lanaway Field), chapter 4 (Ricinus Field) and chapter 6 (Simonette Field), the depositional sequence history will be reviewed below for the Hume-Dawson to the Beaverhill-Saskatchewan subsequences (Moore, 1988 and 1989a) in the Western Canadian Sedimentary Basin (WCSB).

The case studies pertain to the Leduc reefs of the Saskatchewan Group subsequence (Moore, 1988). There are three major subsequences which involve oil producing carbonate reefs; namely the Upper Keg River, Rainbow and Upper Winnipegosis reefs of the Hume-Dawson subsequence, the Swan Hills Fm reefs of the Beaverhill subsequence and the Leduc Fm reefs of the Saskatchewan subsequence. The Devonian history of the WCSB is divided into five major rock sequences; each divided by discontinuities that encompass a period of sea-level rise followed by a fall of sea level and ending in emergence (Moore, 1988). The reef building is pulsatory resulting in the different subsequences.

The first rise of sea level in these reef-building subsequences (Hume-Dawson) occurred during the deposition of the Lower Keg River Member in Northern Alberta and the Lower Winnipegosis unit in Southern Saskatchewan (Brown et al., 1990). As shown in Moore (1988), the Keg River barrier reef (or Keg River - Pine Point barrier reef; Moore, 1989a) formed northeastward of the Peace River Arch. Behind this barrier reef, pinnacles up to 200 m in height grew in the Keg River and Winnipegosis Fms within the Elk Point Basin (see Fig. 5 of Moore, 1988). Transgression at the end of Winnipegosis/Keg River time resulted in basin shallowing and reef growth termination within the resulting hypersaline environment. The basal salt units of the Prairie Fm and the Black Creek Member of the Muskeg Fm were deposited during this time of limited water circulation within the Elk Point Basin. The end of the sequence resulted in further deposition of anhydrites, shales and carbonates followed by the Watt Mountain unconformity. Anderson et al. (1989d) shows examples of Elk Point carbonate reservoir seismic signatures.

The next two subsequences correspond to the Beaverhill Gp (late Givetian to early Frasnian) and the Saskatchewan Gp (mid-Frasnian to end of Frasnian). The depositional history of both of these subsequences contain a carbonate platform development, platform reef growth, basin filling by mixed carbonates and siliciclastics and finally, by progradation of the carbonate platforms (Moore, 1989a).

The Beaverhill Gp subsequence contained the Swan Hills Formation reefs, the Waterways Formation shales and finally the Cooking Lake Formation carbonate platform. The Swan Hills reefs are seismically described in Anderson et al. (1989a) and Ferry (1989). The growth of the Swan Hills reefs was mostly pulsatory and the reefs have been categorized into several cycles of reef "layering" (Wendte and Stoakes, 1982). The progradation of the carbonate platform at the end of the subsequence resulted in the deposition of the lower part of the Cooking Lake Fm. The Peace River Arch was still a positive feature at this time (Chapter 5).

The carbonate platform of the reefs of the Saskatchewan subsequence is either the Cooking Lake Fm or an argillaceous ramp of the Waterways Formation. The Leduc reefs have been divided into three geographical realms in Stoakes and Wendte (1987). The Leduc platform reefs in the southeastern realm include the Bashaw-Duhamel and Rimbey-Meadowbrook reef chains, Ricinus Field and Lanaway Field. These reefs have the Cooking Lake Fm as a platform facies. The reefs of the western region such as the Simonette Field (Chapter 6) are built on the Waterways Fm. The northwestern realm reefs generally fringe the Peace River Arch. Anderson et al. (1989c) shows examples of Woodbend Group reef seismic signatures.

Nisku Fm (Upper Frasnian) reefing occurred in the West Pembina Shale Basin. The reefing in the Nisku Fm may be Zeta Lake member pinnacles or carbonate porosity resulting from drape over the larger Leduc reefs (as in Chapter 3). The basin infill period saw the deposition of the Nisku Fm and Birdbear Fm platform carbonates. The end of the Frasnian is highlighted by an extinction event which may be due to a meteorite impact (Moore, 1988).

3.1.1 Lanaway Field

The Upper Devonian Woodbend Group in central Alberta is subdivided into four formations: Cooking Lake, Duvernay, Leduc, and Ireton. The Cooking Lake represents platform facies. The Leduc is reefal facies; the Duvernay and Ireton are inter-reef shales (Anderson et al., 1989a, b and c; Klovan, 1964; McNamara and Wardlaw, 1991; Moore, 1988, 1989a and b; Mossop, 1972; Mountjoy, 1980; Stoakes, 1980; Stoakes and Wendte, 1987; and Hinds et al., 1994a).

The Leduc Formation at Lanaway (Figs. 3.2 and 3.3) is interpreted to be a large atoll. It towers some 200 m above the Cooking Lake platform and exhibits a seismically mappable (peripheral) raised rim and a structurally lower central lagoonal area. Such raised rims are described in Mossop (1972) in his study of the isolated Leduc Formation limestone reef complex at Redwater. In that study the raised rim was postulated to arise primarily as a result of the greater degree of differential compaction of the central lagoonal facies in comparison to the rigid reef facies. The updip edge (to the northeast) of the raised rim at Lanaway is productive where the reef is structurally closed and effectively sealed by the inter-reef shales of the Duvernay and Ireton Formations (Hinds et al., 1994a). The geologic cross-sections shown in Figures 3.4, 3.5 and 3.6 (from wells shown in Fig. 3.3) and the seismic section (Fig. 3.7, on the seismic line on Fig. 3.3) illustrate the interpreted morphological relationships between the Leduc and inter-reef shales of the Ireton and Duvernay in the Lanaway area.

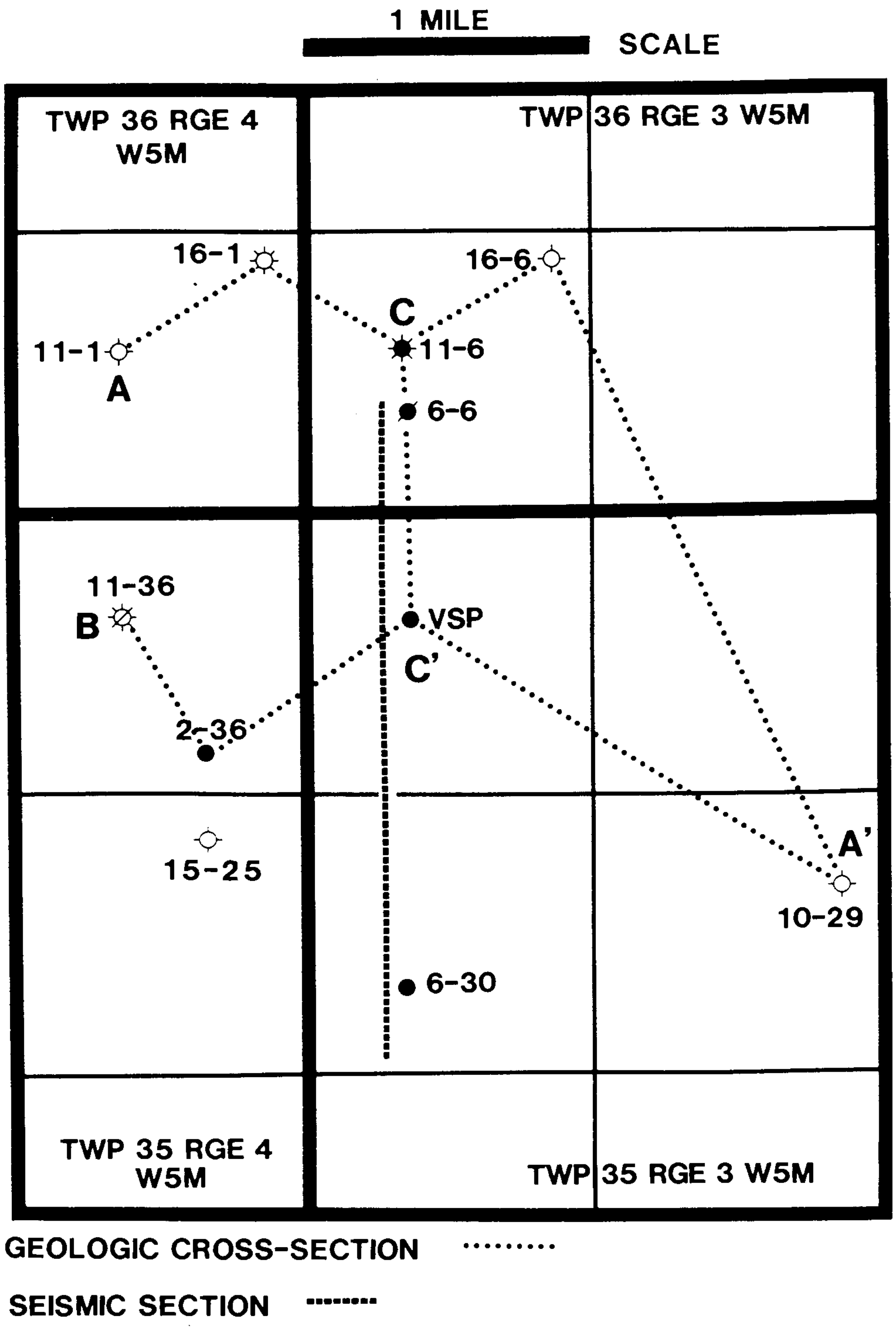

Figure 3.3 Detailed map of the Lanaway study area displaying the seismic section traverse for the seismic data shown in Figures 3.7, 3.8, 3.14 and 3.15 and the locations of the wells used in the geological cross-sections shown in Figures 3.4, 3.5 and 3.6 (from Hinds et al., 1994a and c).

On the surface seismic data, the Lanaway Leduc reef is readily differentiated from inter-reef shales. The carbonate build-up is characterized by appreciable velocity pull-up (25 ms), time-structural drape at the top of the Devonian (25 ms) and character variations within the Woodbend Group (associated with the abrupt transition from shale to reefal facies). Back from the steeply dipping edge, the top of the reef is clearly defined on seismic data, being manifested as a high-amplitude peak on normal polarity data.

The results and interpretations of the 2-D surface seismic and VSP surveys (performed on well C' shown in Fig. 3.3) and the seismic signatures of the top of the Leduc reef at Lanaway are discussed in this chapter. The seismic data were acquired prior to drilling the VSP well, which ultimately ended up intersecting the reef some 80 m below the prognosed depth while the VSP survey was run in an attempt to resolve the apparent discrepancy between the interpreted depth of the reef as derived from surface seismic data and the geology at the exploratory (VSP) well.

3.2 Well Nomenclature

The nomenclature for well locations within the Western Canadian Sedimentary Basin (WCSB) generally comprises a four number reference system (Anderson et al., 1989b). The two numbers (as in the well location 11-1 in Fig. 3.3) are a short form for a more detailed well location system utilized within the WCSB area. The well location system will be described briefly in order to assist the reading of the maps in this and later chapters.

As seen in Figures 3.2 and 3.3, geographical areal units are used in the WCSB referred to as Townships and Ranges. Townships increase in value from South to North and Ranges increase in value (until a Meridian is crossed) from East to West. A single Township and Range involve an area of six by six miles. The Township and Range square is subdivided into thirty-six square units called Sections. Each Section is one mile by one mile in size and is numbered 1 to 36, starting in the southeast corner of the Township and Range square. The smallest sub-division is the land survey division (LSD) which is a quarter mile by quarter mile in size. Within each section, there are sixteen quarter-section LSD's. The LSD numbering starts in the southeast corner of the section. The Ranges are referenced to Meridian lines (lines accurately running north and south through any point on the Earth's surface). After a major Meridian line is crossed, the Range values restart at 1.

As seen in Figure 3.2, the Lanaway Field lies within Ranges 3 and 4 and Township 36 and is west of the fifth Meridian (labelled W5M in Figure 3.2). In Figure 3.3, the two digit well name refers to the LSD and Section numbers. The well 11-1 lies in the 11th LSD of Section 1. The well is geographically tied to the quarter by quarter mile land spacing unit. The full name of the well would be 11-1-36-4 W5M (LSD-Section-Township-Range). For this and the other chapters concerning the case studies, the well name can, at times, be shown in the shortened format as in the example of 11-1.

3.3 Lanaway Field (at the VSP well)

Full Leduc reef at Lanaway Field towers up to 200 m above the Cooking Lake platform and has a structurally lower interior lagoon (Figs. 3.4 and 3.5). Production from the Leduc is

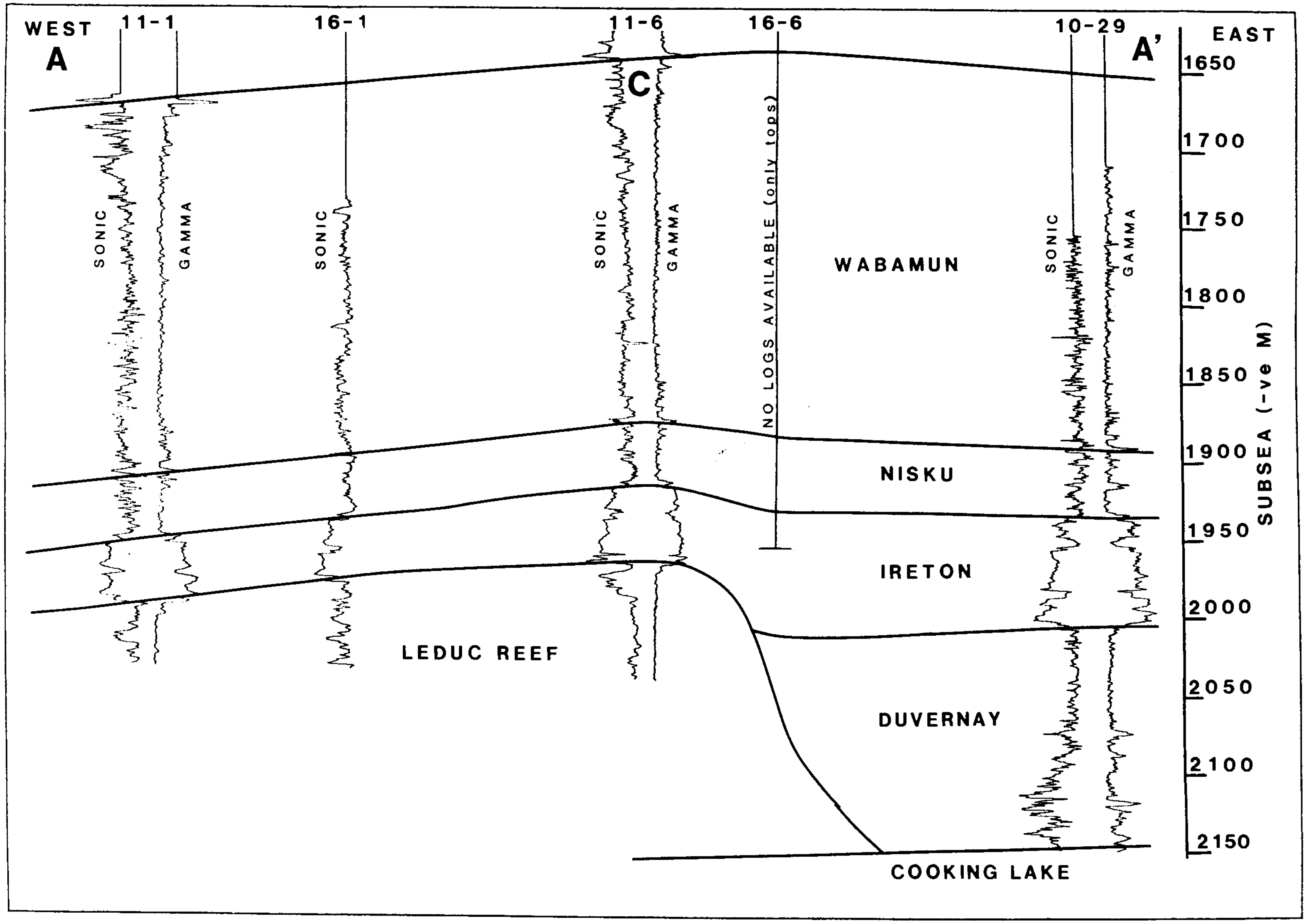

Figure 3.4 West-east geologic cross-section A-A' (refer to Figure 3.3 for well locations). The Leduc Formation reef in well 11-1 is structurally low and wet; wells 16-1 and 11-6 are productive (Leduc oil reservoirs); and wells 16-6 and 10-29 are off-reef and abandoned (from Hinds et al., 1994a and c).

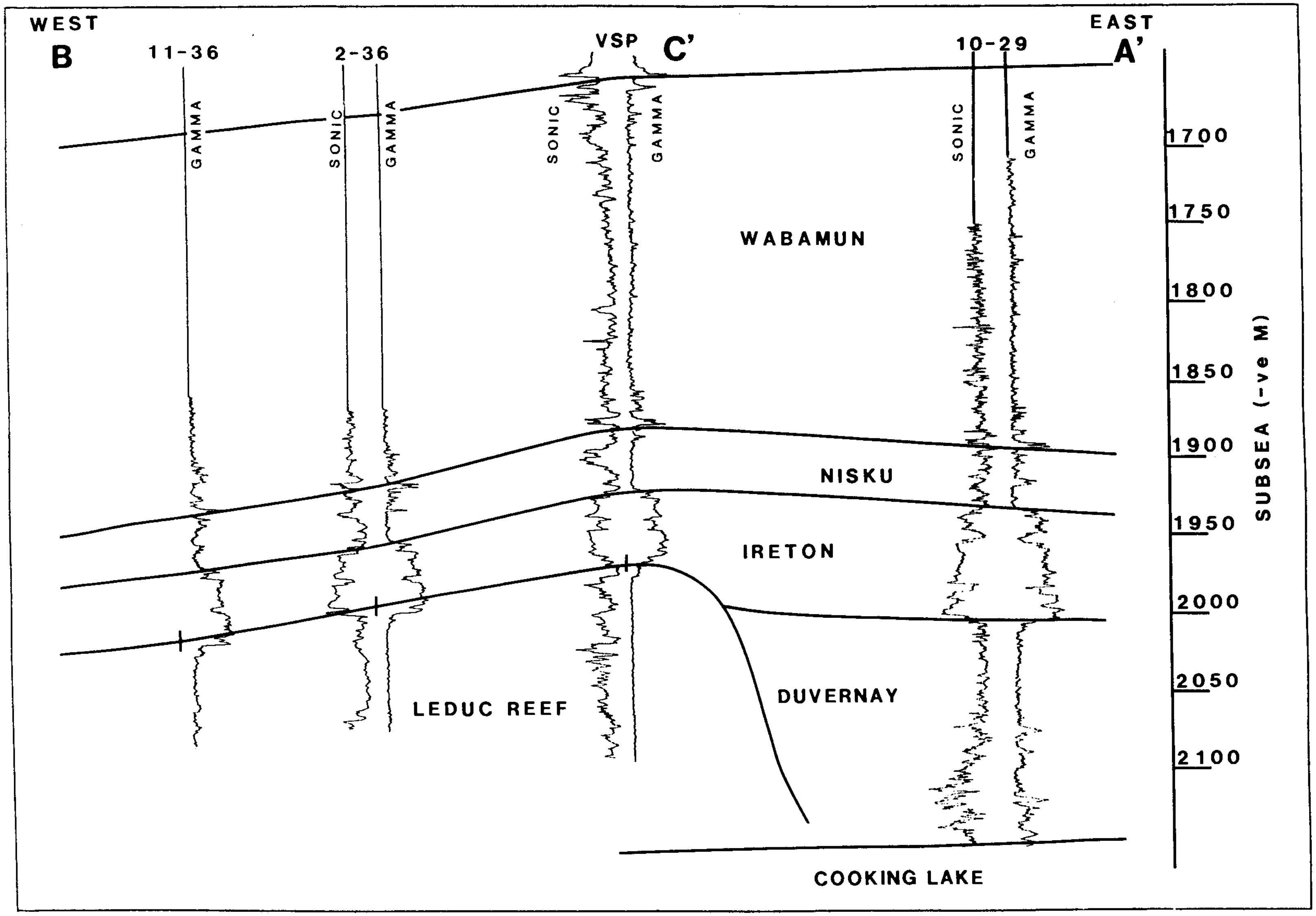

Figure 3.5 West-east geologic cross-section B-A' (refer to Figure 3.3 for location). The Leduc Formation in wells 11-36 and 2-36 (producing oil from the Nisku) is structurally low and wet; the VSP well is productive (Nisku and Leduc Formation oil reservoirs); and well 10-29 is off-reef and abandoned.

restricted to the updip eastern edge (raised rim) of the reef complex (up to 50 m of pay). The eastern and western limits of production are defined by the fore-reef slope and the hydrocarbon/water interface, respectively.

The structural geologic cross-sections (based on the wells located in Fig. 3.3) shown in Figures 3.4, 3.5 and 3.6 illustrate the morphology of the Lanaway complex. Borehole well 10-29 (Fig. 3.4) is off-reef and encountered a full section of inter-reef shale (Ireton and Duvernay); 11-1 is interpreted as having penetrated the structurally low and wet interior lagoon; 16-1 and 11-6 were drilled into the up-dip raised rim of the Lanaway reef and are productive. Well 11-36 (Fig. 3.5) is interpreted as having penetrated the structurally low and wet interior lagoon; 2-36 and the VSP well were drilled into the raised rim of the Lanaway complex. The VSP well is productive. Well 2-36 penetrated the Leduc below the hydrocarbon/water contact; however the well is classified as a Nisku oil well with extended productivity from gas from the Viking Formation of the Cretaceous Colorado Group and oil from the Basal Quartz member of the Ellerslie Formation of the Lower Mannville Group (Lower Cretaceous). These three producing zones (Nisku, Viking and Basal Quartz) are stratigraphically listed in Figures 3.1A-C. The VSP well has a different oil/water contact than 11-6 to the north and, consequently, is assigned to a separate pool. The hydrological barrier between these two wells is related to structural relief at the Leduc level (Fig. 3.6). This relief has been described to be due to several processes or features including surge channels, shale tongues, differential compaction, or original reef morphology by Anderson (1989a, b and c), Klovan (1964) and Mossop (1972).

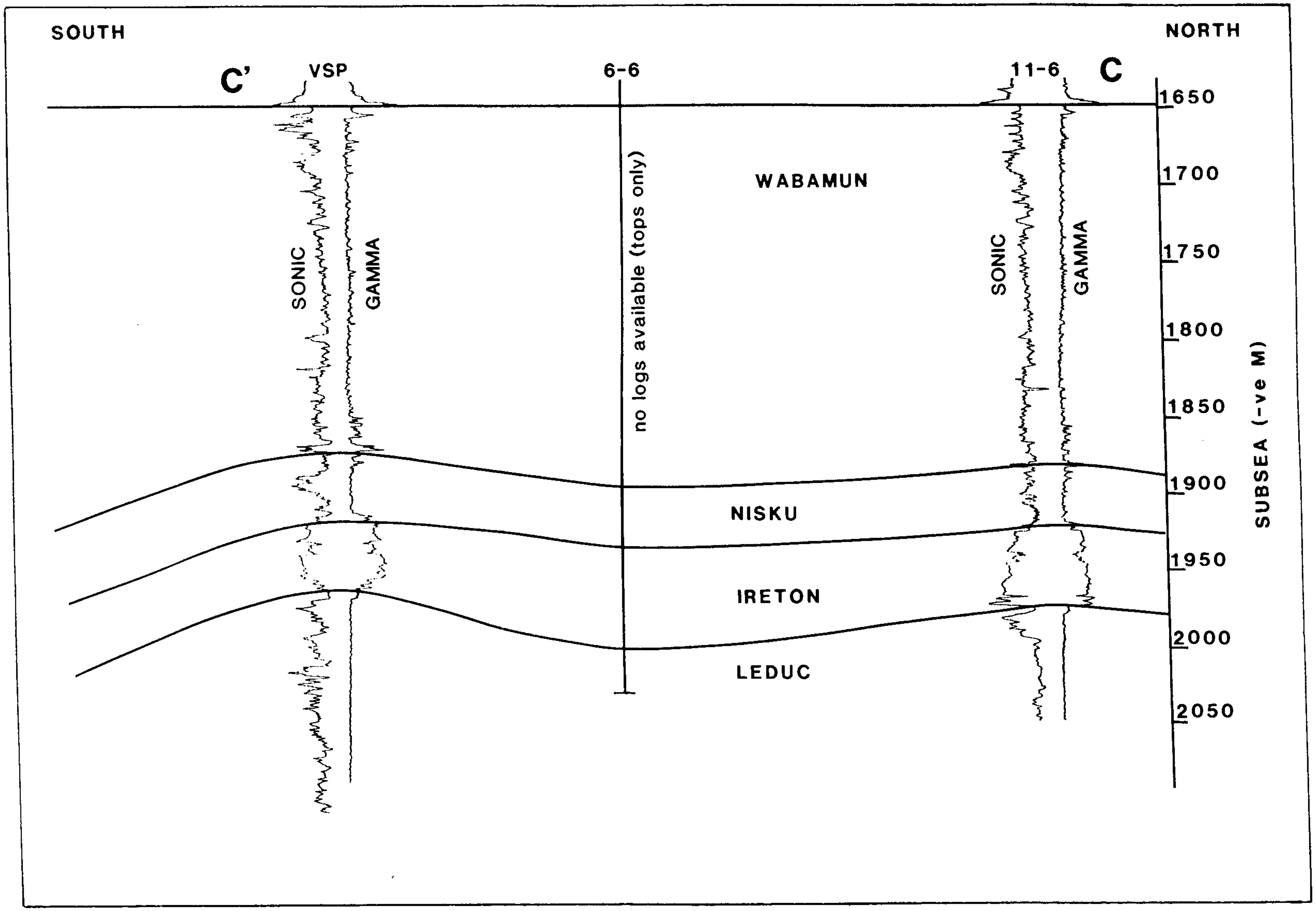

Figure 3.6 North-south geologic cross-section C-C' (refer to Figure 3.3 for location). The Leduc Formation in well 11-6 and the VSP well is productive; and well 6-6 is wet and classified as an abandoned oil well.

The VSP well (Figs. 3.5 and 3.6), although ultimately productive (from both the Nisku and Leduc), was 80 m low at the Leduc level relative to the original seismic prognosis (Hinds et al., 1994a). This pre-drill structural estimate was based on the conventional seismic data interpretation displayed as Figures 3.7 and 3.8. In the original interpretation, the Leduc event is up to 30 ms (80 m) higher between CDP traces 110 and 140 than elsewhere. Geologically, this anomaly was initially envisioned as localized, late stage accretionary reef growth. The drilling of the VSP well however, established that on the original interpretation, the top of the Leduc was miscorrelated by one cycle (between CDP traces 110 and 140). Well log data established that at the VSP well, the Leduc top was more-or-less structurally consistent time-wise with the top of the Leduc elsewhere on the seismic line.

3.4 VSP data acquisition

In an effort to resolve the apparent discrepancy between the surface seismic data (as originally interpreted; Figs. 3.7 and 3.8) and the Leduc top at the VSP well, a VSP survey was designed and conducted at that well site (by myself whilst being employed by Gulf Canada Resources Ltd). The interpretation of the VSP was expected to elucidate:

1) the geological significance (if any) of the misinterpreted seismic anomaly; and

2) the effect of possible multiple interference on the seismic data.

The VSP data were acquired at a single surface offset, located 200 m to the west of the VSP

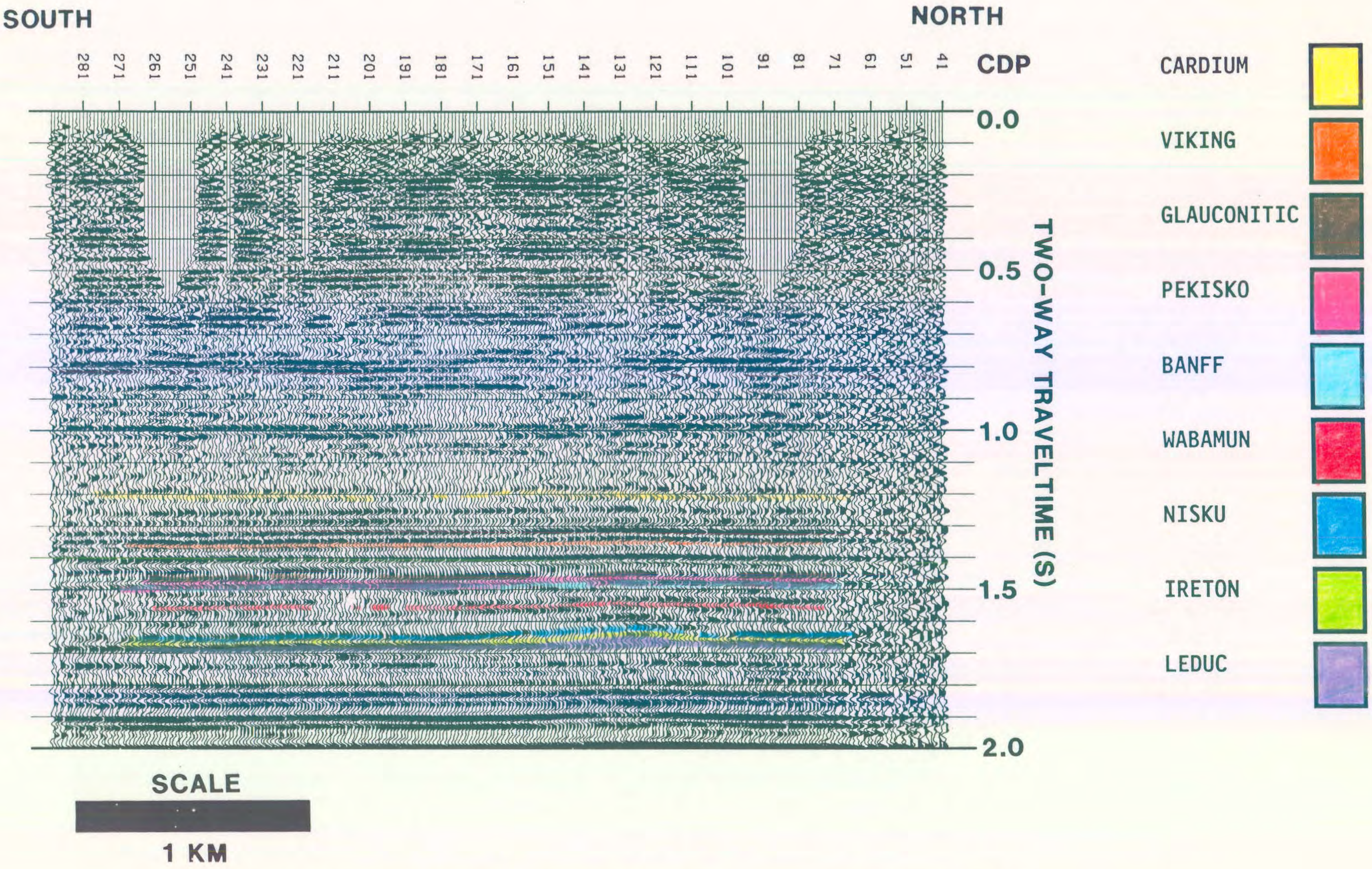

Figure 3.7 North-south oriented example seismic line showing the geophysical interpretation at the VSP well site prior to drilling (refer to Fig. 3.3 for location).

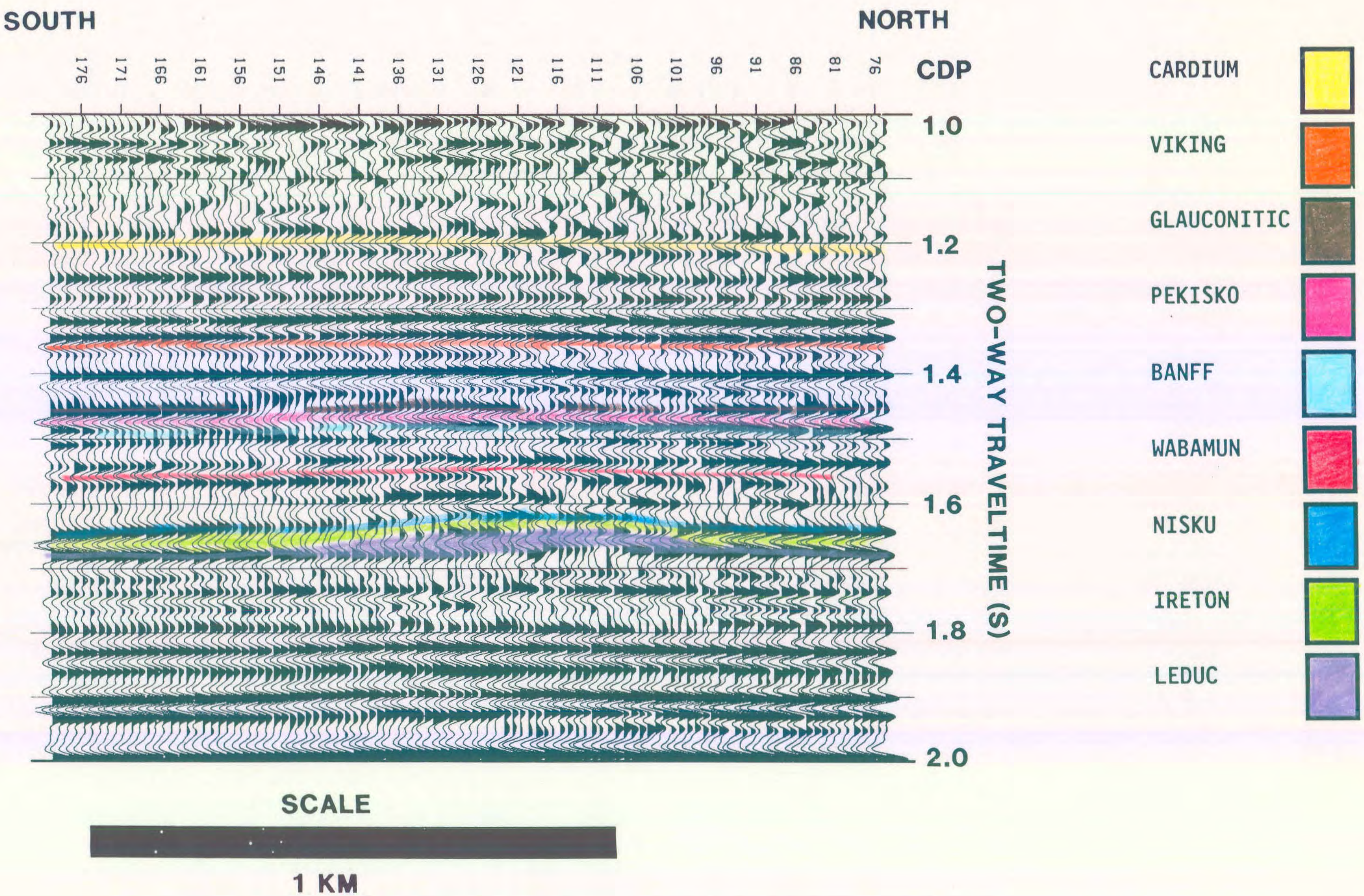

Figure 3.8 Enlarged version of the apparent time-structural anomaly at the Leduc level (shown in Fig. 3.7). The location of the VSP well site is at CDP number 116. (from Hinds et al., 1989a; Hinds et al., 1994a and c).

well on the lease access road. The source consisted of two in-series Vibroseis units utilizing an 8 to 96 Hz input sweep (designed to be compatible with the frequency content of the existing surface seismic data). The Vibroseis sweep was 13 seconds in duration and the recording length was 16 seconds, resulting in a 3 s-long cross-correlated output time series. On average, six sweeps were summed for each subsurface geophone sonde location. The source site was partially frozen and suitable coupling was achieved. The Vibroseis pad location at the offset was shifted periodically by a minor amount to ensure ground coupling stability and to minimize damage to the surface of the lease access road.

The total depth (TD) of the VSP well was 2990 m below the Kelly Bushing (KB) at the time of the running of the VSP survey. The well was drilled slightly further following the survey for stratigraphic evaluation. The elevation of the KB was at 968 m above sea level (asl) and the source at 963 m asl. The geophone sonde was lowered to TD, then raised at 20 m intervals to 2590 m below KB (30 m above the Wabamun Group). Between 2590 and 1315 m (shallowest processed sonde depth location), the sonde recording interval was increased to 25 m. Data were only recorded at three levels above 1315 m (viz at 600, 1000 and 1150 m). These data were acquired principally for sonigram calibration purposes albeit every VSP level first break time and corresponding depth could be used during the sonic log calibration (Hinds et al., 1994c). At each sonde location, the three-component geophone tool was locked in place in the borehole with the locking arm.

The data were recorded at a 2 ms sample interval using the SSC 1078 micro-Vax based system. The recording filter was set at OUT/OUT.

The offset location was chosen to be situated behind a bend in the road so that the source was not in direct line of sight of the well borehole along the lease road (the road was built by the well operator to gain access to the well lease). Another criterion in the choice of the source location was the utilization of a patch of trees that was in the corner of the road between the source and the well which would assist in the reduction of the amplitude of the pseudo-Rayleigh wave propagation along the ground surface thereby aiding in the elimination of groundroll induced interference (tube waves) with the downgoing and upgoing signal.

3.5 VSP interpretive processing

As an aid to the interpretation of the VSP data a suite of interpretive processing panels (IPP's) were generated for these data (Hinds et al., 1989a, Hinds et al., 1991a, 1991b and 1993c, Hinds, 1991c, Hinds et al., 1993a, Hinds et al., 1993b, 1994a and 1994c). The panels allowed the progressive interpretation of the data in order to facilitate the quality control of the processing sequence. More specifically the panels displayed:

1) up- and downgoing P-wavefield separation

2) deconvolution of the separated upgoing P-waves using an inverse filter calculated from the separated downgoing P-waves; and

3) inside and outside corridor stacks of both the deconvolved and nondeconvolved upgoing P-waves.

3.5.1 P-wave separation to output Z_{up}(+TT) data

In the initial phase of processing, the upgoing and downgoing P-waves of the vertical geophone data, **Z(FRT)**, were separated. This separation procedure is illustrated in the wavefield separation IPP (Hinds et al., 1989a and Hinds et al., 1994c) in Figure 3.9.

The **Z(FRT)** data after trace normalization and the gained **Z(FRT)** data are displayed in panels 1 and 2 of Figure 3.9. Several primary upgoing reflections can be identified on these data: viz Viking (at a depth of 2100 m); Mannville (the Glauconitic at 2158 m); and Banff (2293 m). Note that the series of strong reflections that originate below the VSP well TD do not intersect the first break curve, and therefore cannot be confidently classified as either primary or multiple events (Hinds et al., 1989a and Hinds et al., 1994c).

The gained **Z(-TT)** data in panel 3 illustrate that the downgoing wavetrain (the multiples) is comprised mostly of high amplitude surface-generated and less prominent interbed multiples. Surface-generated multiples are recorded on all of the traces and are manifested as laterally continuous events that arrive after the first break events. Interbed multiples, in contrast, do not extend over the entire depth range. If present, they would be present on the deeper traces only (Hinds et al., 1989a).

The downgoing waves contained in panel 3 were separated from the combined wavefield data using an eleven-point median filter and displayed in panel 4, $\mathbf{Z_{down}}$**(-TT)**. The residual upgoing wave content in the $\mathbf{Z_{down}}$**(-TT)** data of panel 4 is minimal. The upgoing waves,

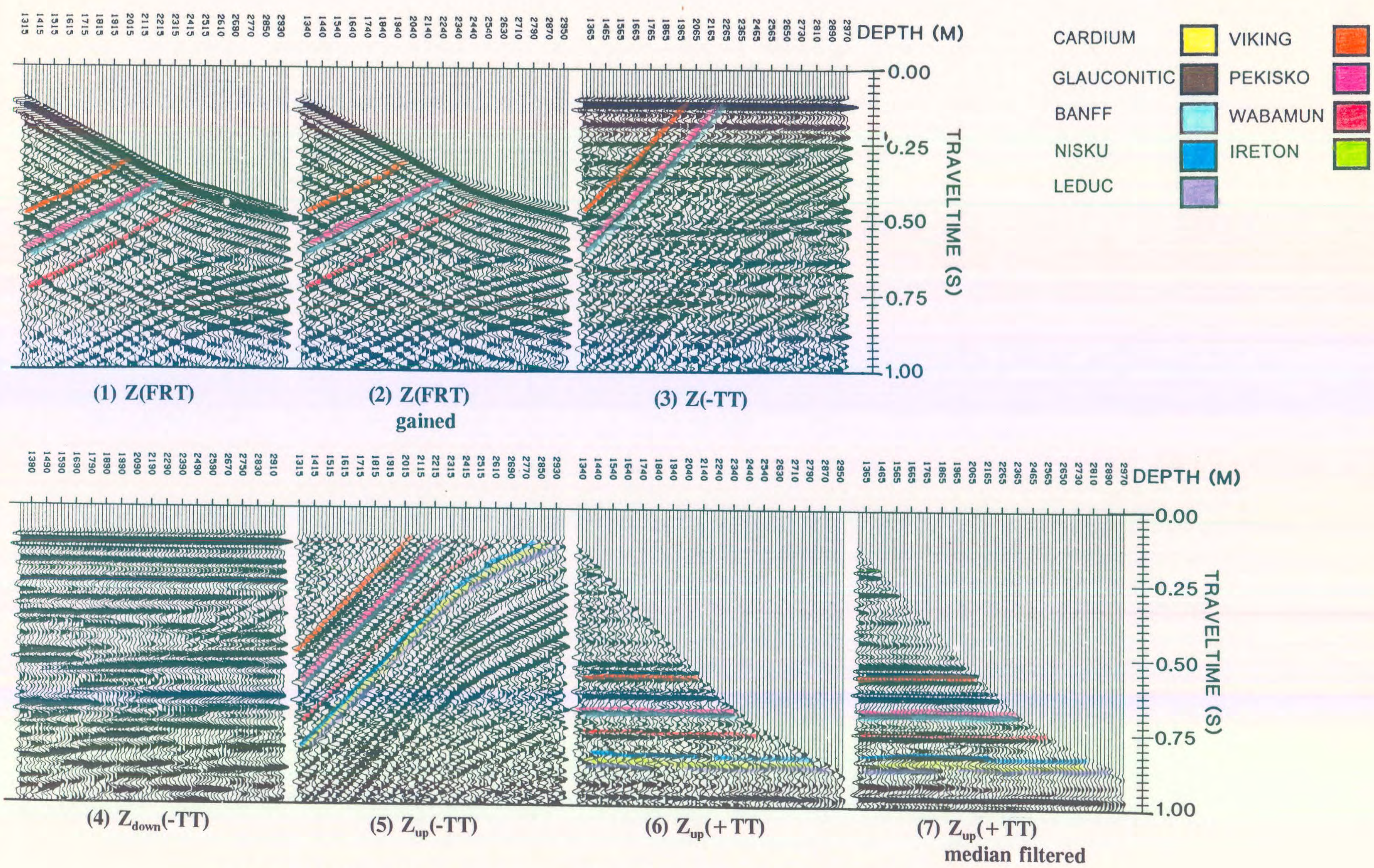

Figure 3.9 Interpretive processing panel depicting the wavefield separation of the near offset VSP data (from Hinds et al., 1989a; Hinds et al., 1994a and c)

$\mathbf{Z_{up}}$**(-TT)** in panel 5, were separated by subtracting a scaled version of the downgoing wavefield, $\mathbf{Z_{down}}$**(-TT)** of panel 4, from the combined wavefield, **Z(-TT)** of panel 3, following the methodologies described by Balch and Lee (1984), Hardage (1985), Hinds et al., 1989a, Hinds et al., 1994c and others. The two final panels (6 and 7) in the wavefield separation IPP display the separated upgoing waves, $\mathbf{Z_{up}}$**(+TT)**, before and after the application of a three-point median filter. The equalized amplitudes of the Cardium, Viking, Glauconitic, Pekisko, Banff, Wabamun, Nisku, Ireton and Leduc events in **+TT** time configuration are interpreted in the final panel and confirmed on the previous panels.

Successful wavefield separation is critical to the interpretation of the VSP data, for any residual upgoing wavefield in the $\mathbf{Z_{down}}$**(-TT)** data in panel 4, will be subtracted out of the upgoing wave data. Note that the median filter (panels 4 and 5) has not been particularly effective in separating those upgoing waves that arrive after the first break time on the deepest sonde location trace (panel 4). This is acceptable however only because these events are below the zone of interest.

3.5.2 VSP deconvolution

Surface-generated and interbed multiples are totally represented on the separated downgoing wavetrain shown in panel 4 of Figure 3.9. The initial downgoing pulse (except in the case of head wave contamination) is the primary downgoing P-wave; any downgoing waves that arrive later are a result of multiple reflections. These multiple events can be effectively removed by deconvolving the upgoing wave data with an inverse filter derived from an analysis of the downgoing wavetrain (Hinds et al., 1989a). The deconvolution IPP shown in Figure. 3.10, as reviewed in chapter 2, enables the interpreter to control the quality of the VSP (up/down) deconvolution process (Hinds et al., 1994c). Panels 1, 2, 6 and 7 in Figures 3.9 and 3.10 are bulk time shifted to facilitate the IPP display.

The first two panels (Fig. 3.10) are the unfiltered and median-filtered $\mathbf{Z_{up}(+TT)}$ data. Panels 3 and 4 are the nondeconvolved **Z(-TT)** and $\mathbf{Z_{up}(-TT)}$ data. The fifth panel is the deconvolved upgoing combined wavefield data, $\mathbf{Z_{(decon)}(-TT)}$, and represents an example of downgoing wavefield deconvolution applied to the combined (total) wavefield as first reported in Smidt (1989). The data following the deconvolution step were then wavefield separated, normalized around the first breaks and then corrected for spherical divergence. The deconvolved data were thereafter time shifted to pseudo-two-way traveltime and the resultant $\mathbf{Z_{up(decon)}(+TT)}$ data are displayed in panel 6. A comparison of the median-filter-enhanced nondeconvolved ($\mathbf{Z_{up}(+TT)}$ in panel 2) and deconvolved upgoing ($\mathbf{Z_{up(decon)}(+TT)}$ in panel 7) wavefield data indicates that the deconvolution process has enhanced the frequencies of the upgoing waves and yet preserved the integrity of the primary reflections.

The effect of the interference by multiples and the relative success of the deconvolution operator, can be appreciated by the analysis of the VSP Glauconitic event. In the $\mathbf{Z_{up}(+TT)}$ data in panel 2 (Fig. 3.10), the nondeconvolved Glauconitic event is relatively continuous at sonde depths below the Cardium (1825m). At shallower depths, the Glauconitic event is partially masked by a possible interbed multiple that has as its lower generating surface, the top of the Cardium. On the $\mathbf{Z_{up(decon)}(+TT)}$ data in panel 7, the Glauconitic event is relatively continuous at all the sonde depths implying that the interfering multiple event has

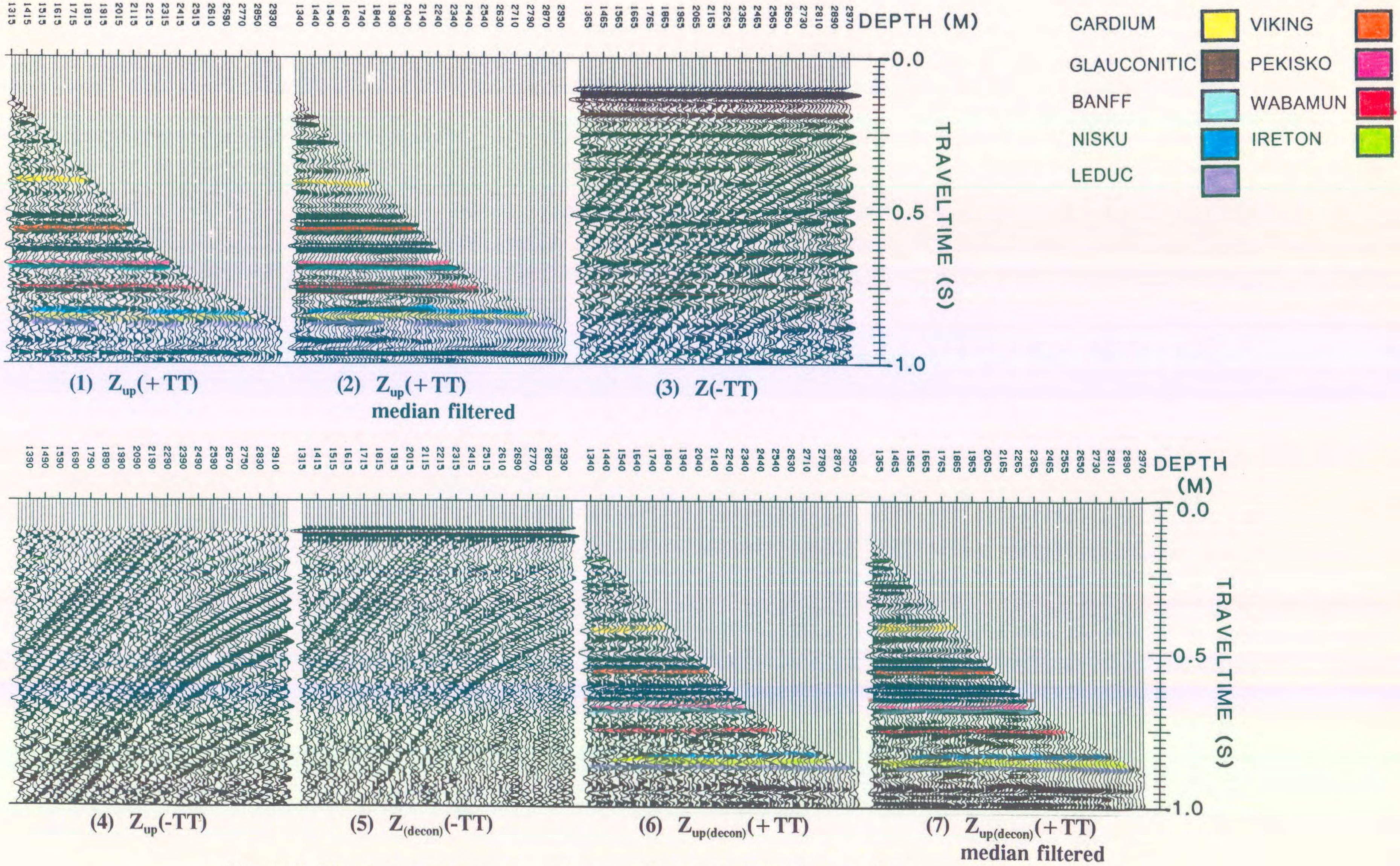

Figure 3.10 Interpretive processing panel depicting the deconvolution of the near offset VSP data (from Hinds et al., 1989a; Hinds et al., 1994a and c).

been attenuated.

Note that the Nisku and Leduc events are relatively low amplitude (in comparison to the Nisku and Leduc events on the seismic line away from the VSP well site) possibly as a result of destructive multiple interference. On the $\mathbf{Z_{up}(+TT)}$ data (panels 1 and 2), a strong peak exists just above (overlapping) the Nisku event from the shallowest trace out to the 2140 m trace. The Nisku event is low amplitude in comparison. After deconvolution, the Nisku event on the $\mathbf{Z_{up(decon)}(+TT)}$ data is laterally continuous in amplitude. The anomalous multiple-induced peak before the deconvolution can be estimated to be up to 5 ms higher than the overlapped Nisku event.

3.5.3 Inside and outside corridor stacks

Multiple contamination on the VSP upgoing waves can be closely examined using the inside and outside corridor stacks of both the $\mathbf{Z_{up}(+TT)}$ and $\mathbf{Z_{up(decon)}(+TT)}$ data. The inside corridor stack of the $\mathbf{Z_{up}(+TT)}$ data contains both the primary and multiple events, whereas the outside corridor stack data should be relatively free of multiples. If the deconvolution is successful in removing the multiples, then both the inside and outside corridor stacks for the $\mathbf{Z_{up(decon)}(+TT)}$ data will be predominated by primary reflections (Hinds et al., 1989a and Hinds et al., 1994c).

In Figure 3.11, the outside and inside corridor stacks are shown in panels 3 and 4, respectively. The input data that are stacked to create the inside and outside corridor stacks are shown in panels 2 and 5. The $\mathbf{Z_{up}(+TT)}$ data shown in panels 1 and 6 are placed beside

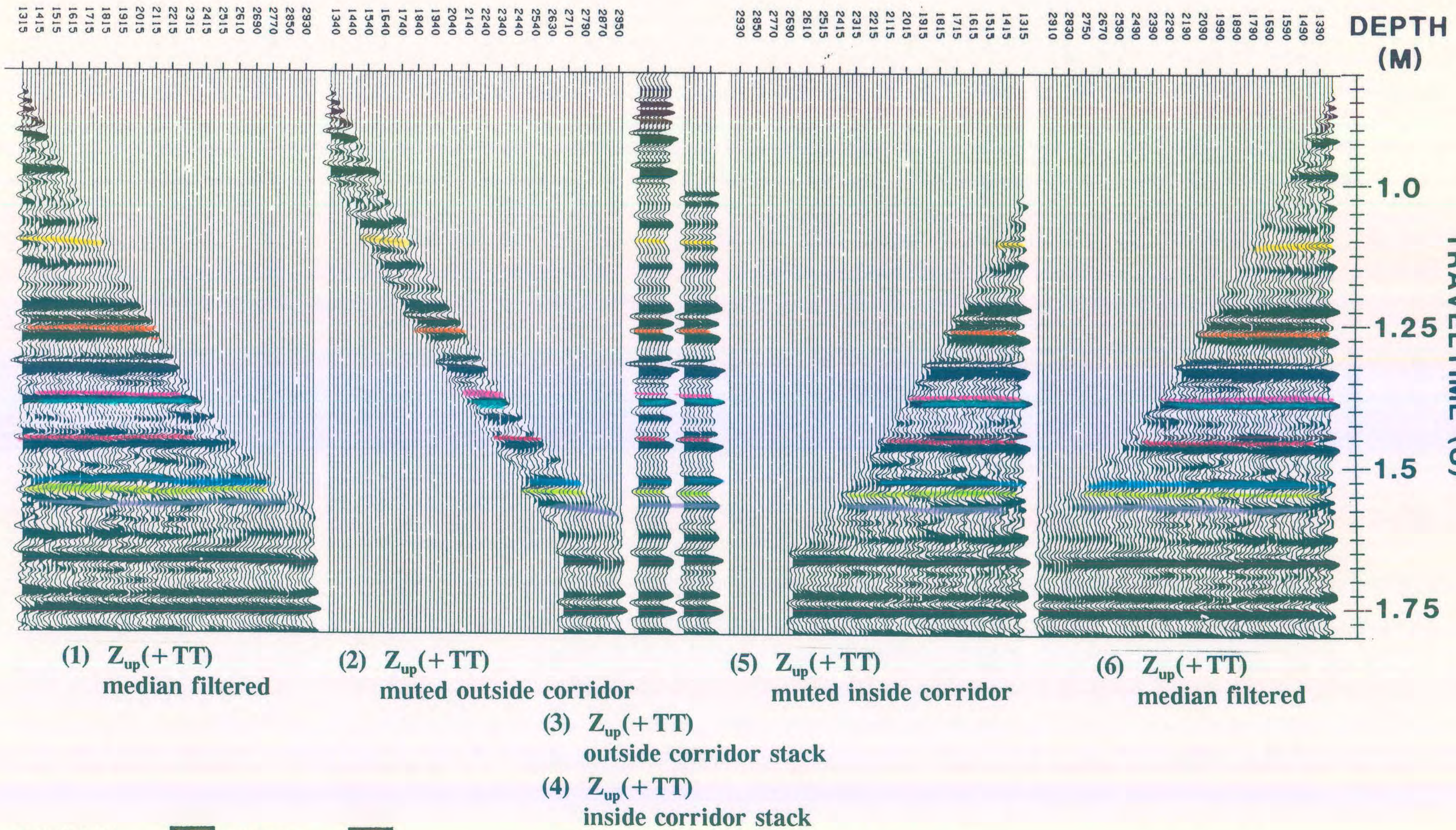

Figure 3.11 Interpretive processing panel illustrating the utility of the nondeconvolved inside and outside corridor stacks for the near offset VSP data (from Hinds et al., 1989a; Hinds et al., 1994a and c).

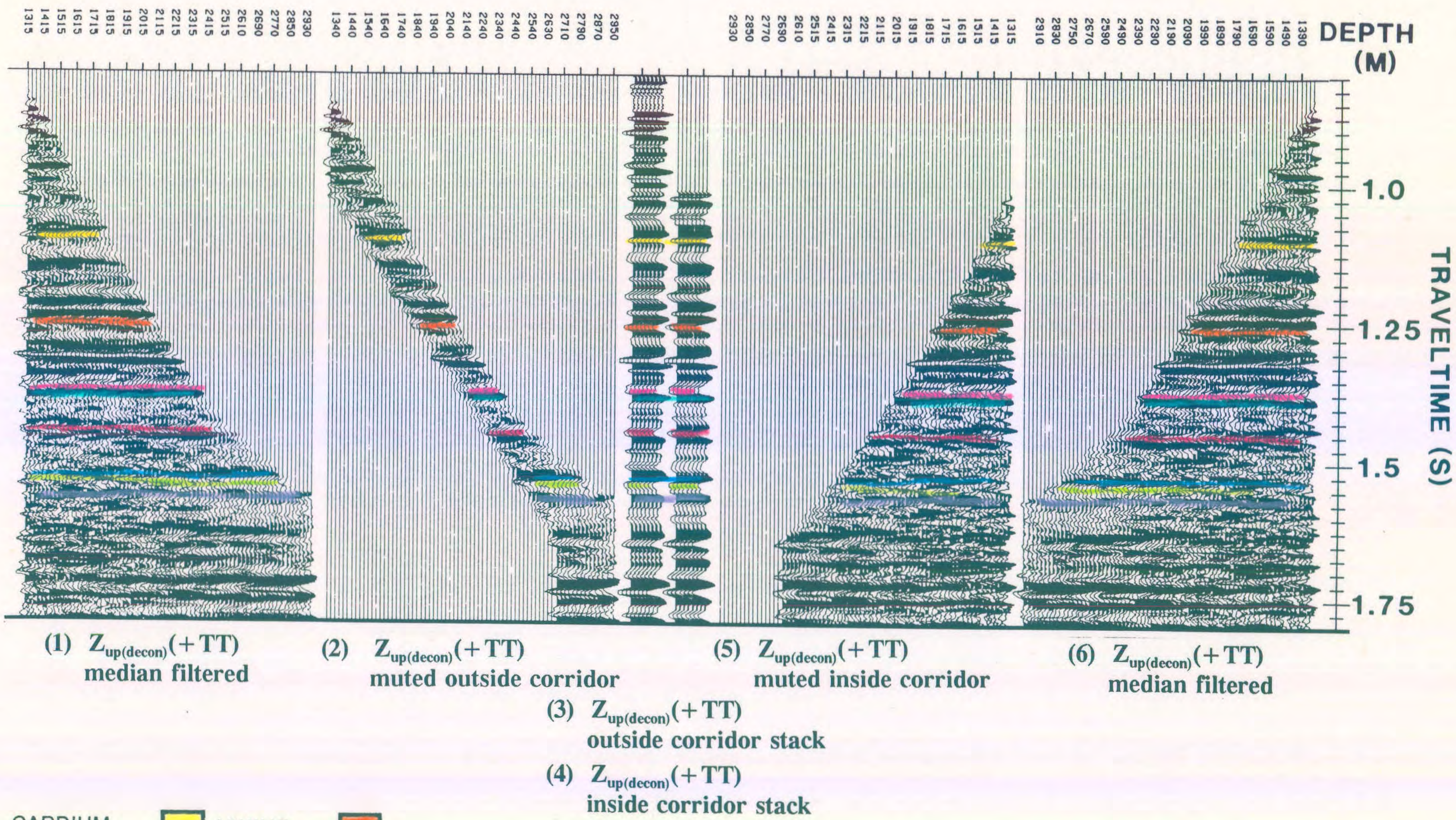

Figure 3.12 Interpretive processing panel illustrating the utility of the deconvolved inside and outside corridor stacks for the near offset VSP data (from Hinds et al., 1989a; Hinds et al., 1994a and c).

the corridor muted $\mathbf{Z_{up}}$**(+TT)** data of panels 2 and 5 to show what has been muted.

The inside and outside corridor stacks (panels 4 and 3, respectively) differ below both the Cardium and Banff (at the Wabamun, Nisku and to a lesser degree at the Leduc events) suggesting that multiple interference occurs within these zones. An explanation is that the noticeable effect of the multiples contaminating the inside corridor stack is not represented within the outside corridor stack (Hinds et al., 1994a).

A comparison of the $\mathbf{Z_{up(decon)}}$**(+TT)** data inside and outside corridor stacks (Fig. 3.12), indicates that multiple interference was substantially attenuated by deconvolution. More specifically, note that the inside and outside corridor stacks of the $\mathbf{Z_{up(decon)}}$**(+TT)** data are similar, suggesting that deconvolution has effectively attenuated the multiple contamination evident on the inside corridor stack of the $\mathbf{Z_{up}}$**(+TT)** data (panel 1; Fig. 3.11).

3.6 Integrated interpretation

The reinterpreted conventional surface seismic line incorporating the VSP results (Figs. 3.7, 3.8, 3.14, and 3.15) is displayed on the left-hand side of Figure 3.13. A synthetic seismogram for the VSP well, the $\mathbf{Z_{up}}$**(+TT)** data inside corridor stack, and the $\mathbf{Z_{up(decon)}}$**(+TT)** data outside corridor stack are time-tied to the seismic line at the VSP well site (CDP number 127). The inside and outside corridor stacks and the synthetic seismogram, juxtaposed between the two separated parts of the seismic section at the VSP well location, allows a comparison between the three methods of the time-tie to the Leduc surface seismic event.

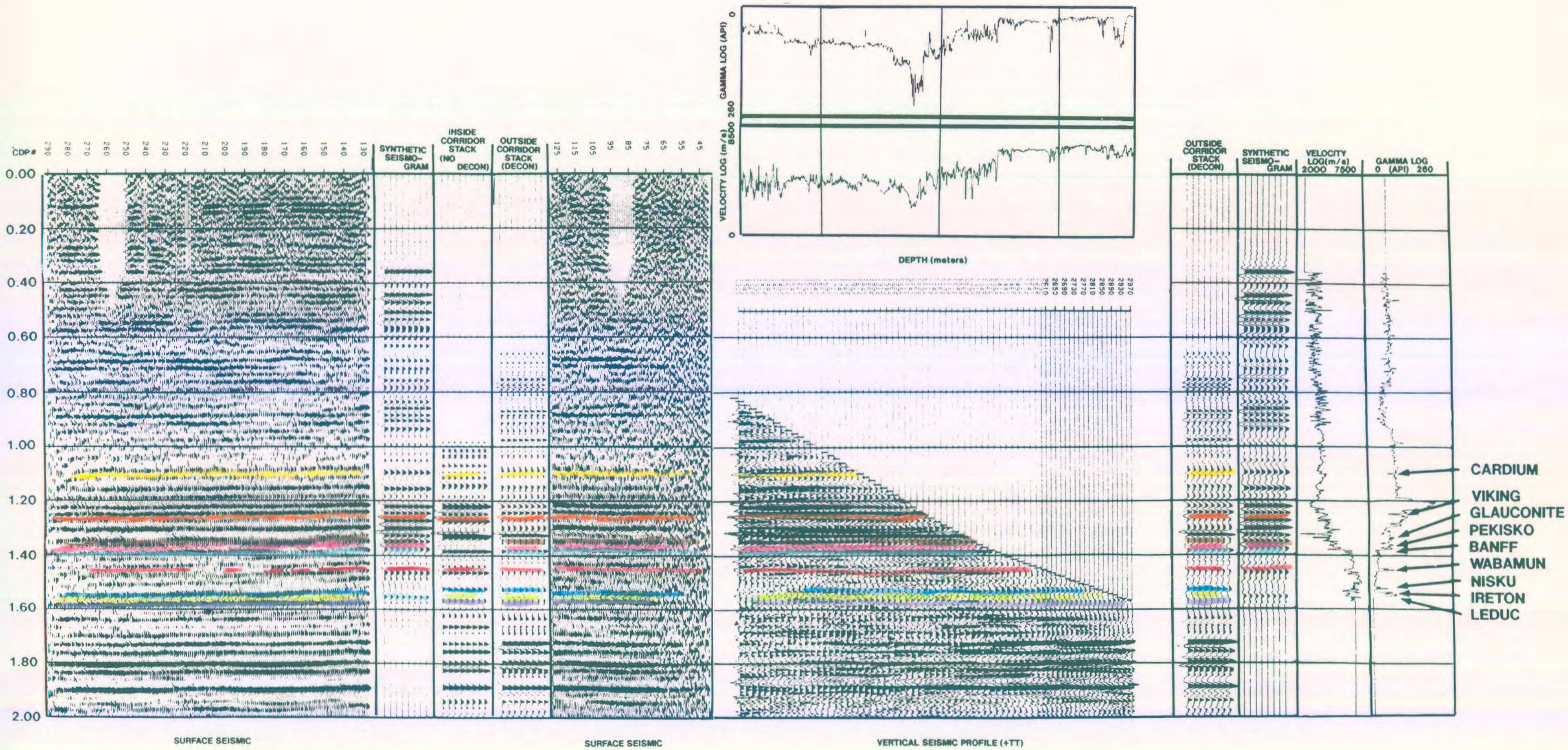

Figure 3.13 Integrated interpretive display (IID) showing the interpretation of the available exploration data for the Lanaway Field case study. The synthetic seismogram was generated using a zero-phase, 30 hz centre frequency Ricker wavelet (from Hinds et al., 1989a; Hinds et al., 1994a and c).

On the right-hand side of Figure 3.13, the VSP data are time-tied to the seismic line, the $\mathbf{Z_{up(decon)}(+TT)}$ data outside corridor stack, the VSP well synthetic seismogram, the VSP well velocity log, and the VSP well gamma ray log. The horizontal scale (depth axis) of the VSP display, $\mathbf{Z_{up(decon)}(+TT)}$, and the scale used for the horizontally-oriented VSP well sonic and gamma ray log depth displays are the same. The outside corridor stack (containing predominantly primary events), the synthetic seismogram, and the two well logs (converted to time) allows for the comparison of the corridor stack, the synthetic seismogram, and the well log data. Because the synthetic seismogram is calculated from the sonic log (where the sonic data are virtually collected continuously) in the same area, the synthetic will have higher resolution than the corridor stack. Since the range of the wavelengths contained in the $\mathbf{Z_{up(decon)}(+TT)}$ data are the same as for surface seismic, in most cases the outside corridor stack interpretation will tie to the seismic data interpretation more closely.

The VSP well sonic and gamma logs are displayed in depth and plotted immediately above the $\mathbf{Z_{up(decon)}(+TT)}$ data in Figure 3.13. The correlation between these data can be illustrated by considering the top of the Wabamun.

Lithologically, the top of the Wabamun in the VSP well is represented by the shale/carbonate contact at a depth of 2616 m. Within the VSP data, there are recorded VSP traces at 2610 m and then below the Wabamun formation top is at 2630 m. The Wabamun event is therefore identified as the trough (some interpreters prefer to use the zero-crossing) located in time between the first breaks for the 2610 and 2630 m sonde depths (approximately 1450 ms). In a similar fashion, the other VSP upgoing events can be identified and then correlated directly to the surface seismic line at CDP number 127, the nondeconvolved inside corridor stack, the deconvolved outside stack, and the synthetic seismogram, velocity and gamma log (displayed in time) for the VSP well.

The location of the Leduc event is of the greatest interest to the interpreter. Note that this reflection, on the surface seismic and VSP data at the VSP well site, is a half cycle lower than initially interpreted by the owners of the data (pre-VSP interpretation shown in Figs. 3.7 and 3.8). The revised surface seismic interpretation is presented in Figures 3.14 and 3.15. A correlation of the VSP and the surface seismic data indicates that the Leduc top was incorrectly identified at the VSP well site on the pre-VSP interpretation. This miscorrelation explains why the Leduc top came in 80 m low relative to prognosis; however, it does not explain why the surface seismic line was originally misinterpreted. Anomalous Nisku, Ireton and Leduc surface seismic signatures between CDP numbers 90 to 140 may have resulted in a misleading interpretation (Figs. 3.14 and 3.15).

This seismic package from the Wabamun to the Leduc events is characterized by:

1) positive time-structural relief (of the order of 5 ms) along both pre-Leduc and deeper post-Leduc events;

2) an anomalously low-amplitude Leduc event; and

3) an anomalous reflection pattern within the Wabamun/Leduc interval (drape over the reef edge by the Wabamun and the Nisku events).

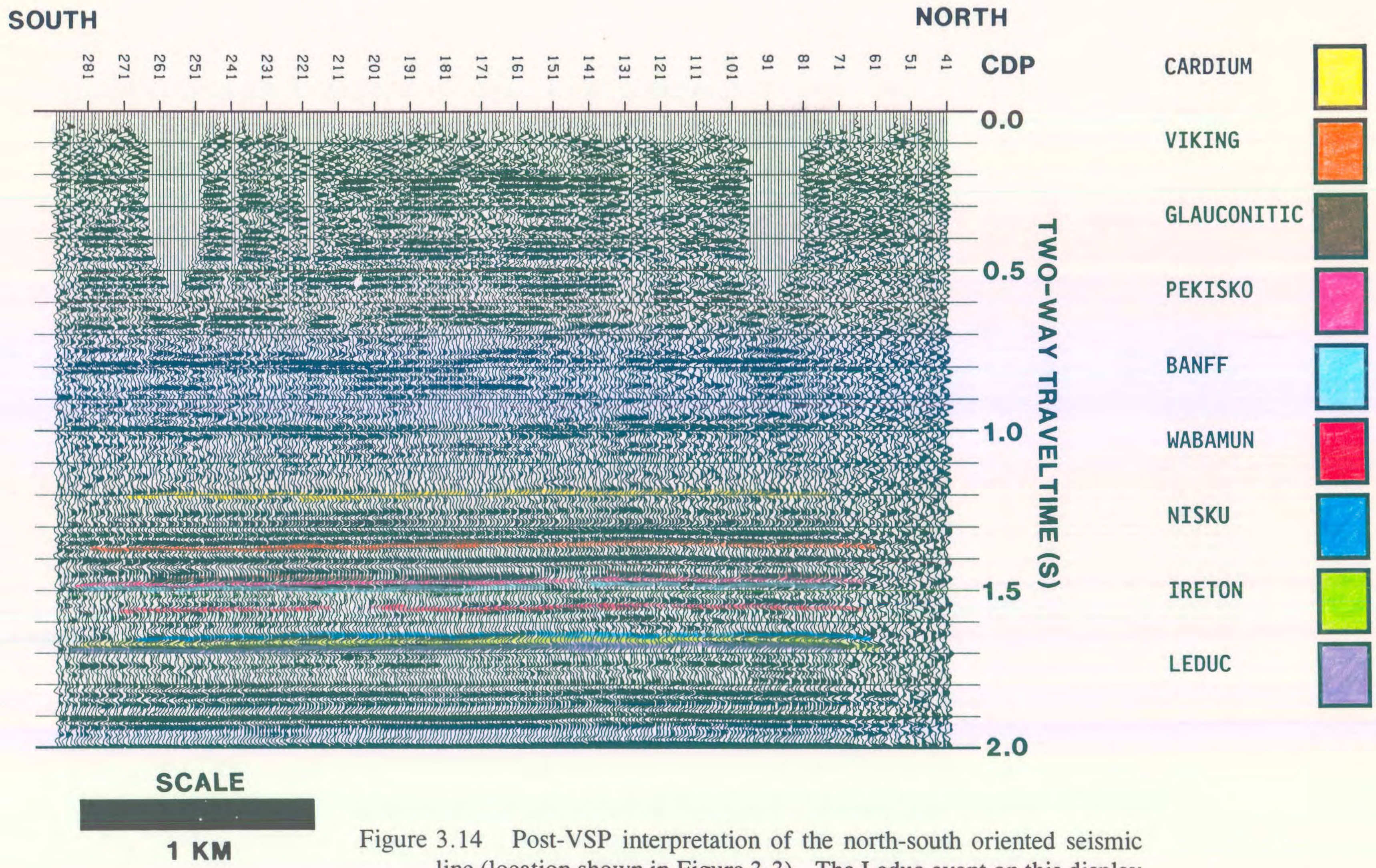

Figure 3.14 Post-VSP interpretation of the north-south oriented seismic line (location shown in Figure 3.3). The Leduc event on this display is only slightly time-structurally elevated at the VSP well site and the updated interpretation is consistent with well log control (from Hinds et al., 1989a; Hinds et al., 1994a and c).

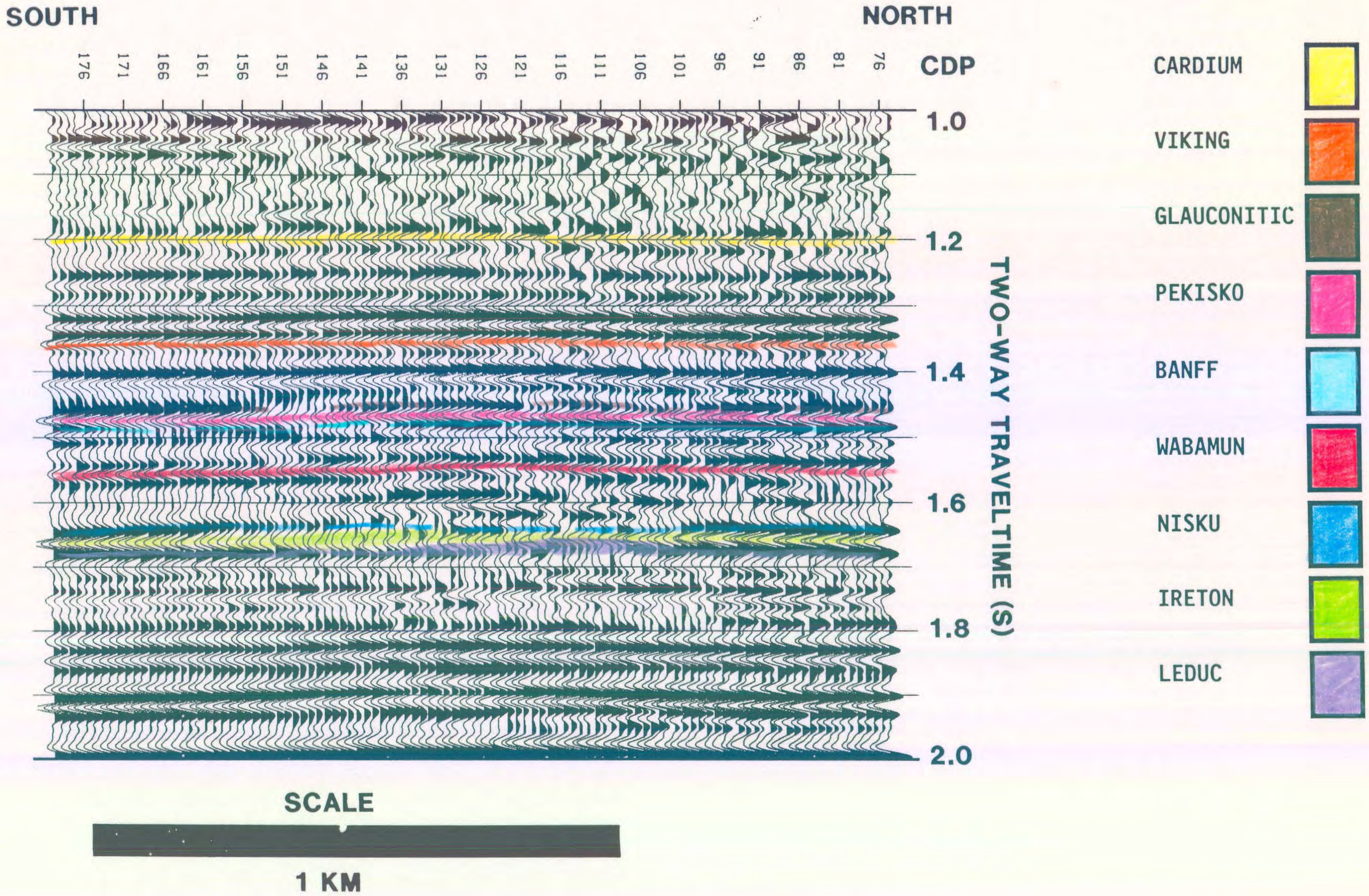

Figure 3.15 Enlarged version of the post-VSP interpretation of the north-south oriented seismic line (shown in Fig. 3.14). The VSP well location is at CDP number 116 (from Hinds et al., 1989a; Hinds et al., 1994a and c).

These three types of seismic signatures were initially interpreted to be diagnostic of the reef and were attributed to an envisioned 80 m of anomalous accretionary reef growth. The time-structural relief in particular was attributed to velocity pull-up and drape, respectively.

The VSP well dataset conclusively established that the Leduc was misidentified on the original interpretation (Figs. 3.7 and 3.8) and that the observed seismic anomalies are not related to late stage accretionary reef growth (Hinds et al., 1994a). There appear to be three most probable candidates for the explanation for the seismic anomaly:

1) structural relief at the Pekisko and Shunda pre-Cretaceous subcrops;

2) stratigraphic anomalies (possible patch carbonate reef) within the Winterburn Group (Fig. 3.1c); and

3) structural thinning of the Ireton near the reef crest (as shown in Fig. 3.6).

Dealing with the first explanation, it is conceivable that the observed anomaly is partially caused by erosional relief at the pre-Cretaceous subcrop (Pekisko and Shunda). As illustrated by the velocity log (Fig. 3.13), the velocity of seismic wave propagation of the Shunda and Pekisko Formations are higher than those of the overlying Cretaceous sediment. Positive erosional relief at the Shunda/Pekisko level would cause pre-Cretaceous events to be time structurally "pulled-up", and the overlying seismic events would appear to be anomalously draped as a result of compaction of the formations above the Pekisko and Shunda material (Anderson et al., 1989a). However, no Shunda Formation material was intersected at the

VSP well in comparison to 14 m at the 6-6 well location (as shown in the Shunda isopach map in Fig. 3.16). The combined Shunda/Pekisko thicknesses at the VSP well and 6-6 are 43 and 55 m, respectively.

The second suggested explanation for the observed time-structure and amplitude anomalies is a lithologic variation within the Winterburn Group. It is possible that a localized Nisku Formation (Winterburn Group) patch reef has developed above the crest of the underlying Leduc reef (similar to the patch reef suggested in the case study in Rennie et al., 1989). The envisioned carbonate build-up would be characterized by a velocity pull-up, time-structural drape, and a character change within the Winterburn Group. Unfortunately, due to the absence of core control within the Winterburn Group, this suggestion cannot be confirmed or negated; however it should be noted that the VSP well and well 6-6 intersected 47.4 and 39.3 m of Nisku, respectively. The added Nisku build-up and corresponding porosity could conceivably contribute to the observed time-structural anomaly. The patch reef could have resulted from the localized structural high resulting from the presence of the reef edge.

The third possibility suggested is that subtle draping of Ireton sediments above the reef crest at the VSP well as has already been highlighted in the north-south geologic cross-section shown in Figure 3.6 could be the cause of the misinterpretation. The isopach map of the Ireton in Figure 3.17 shows that the north-south oriented seismic line (Figs. 3.7 and 3.8) traverses a thick succession of Ireton shales at well 6-6 (66 m), while it is relatively thinner over the reef crest at the VSP well (43 m) and it thickens in LSD 30 towards well 6-30.

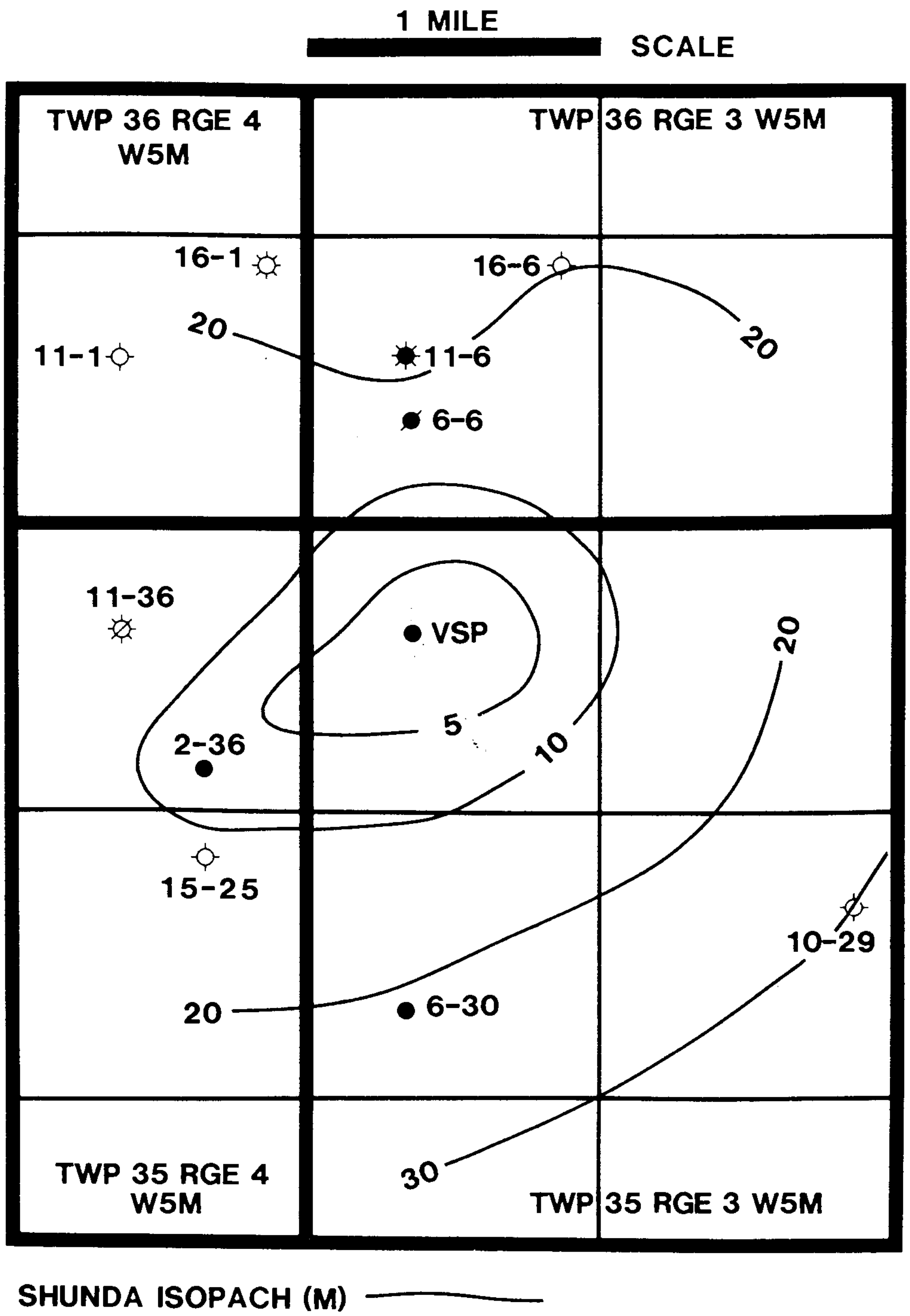

Figure 3.16 Shunda isopach map showing the absence of Shunda at the VSP well. The pre-Cretaceous anomaly may reflect only to a minor to negligible degree a possible source of the seismic defocussing seen on the seismic image of the Ireton to Leduc events at the VSP well (from Hinds et al., 1994a and c).

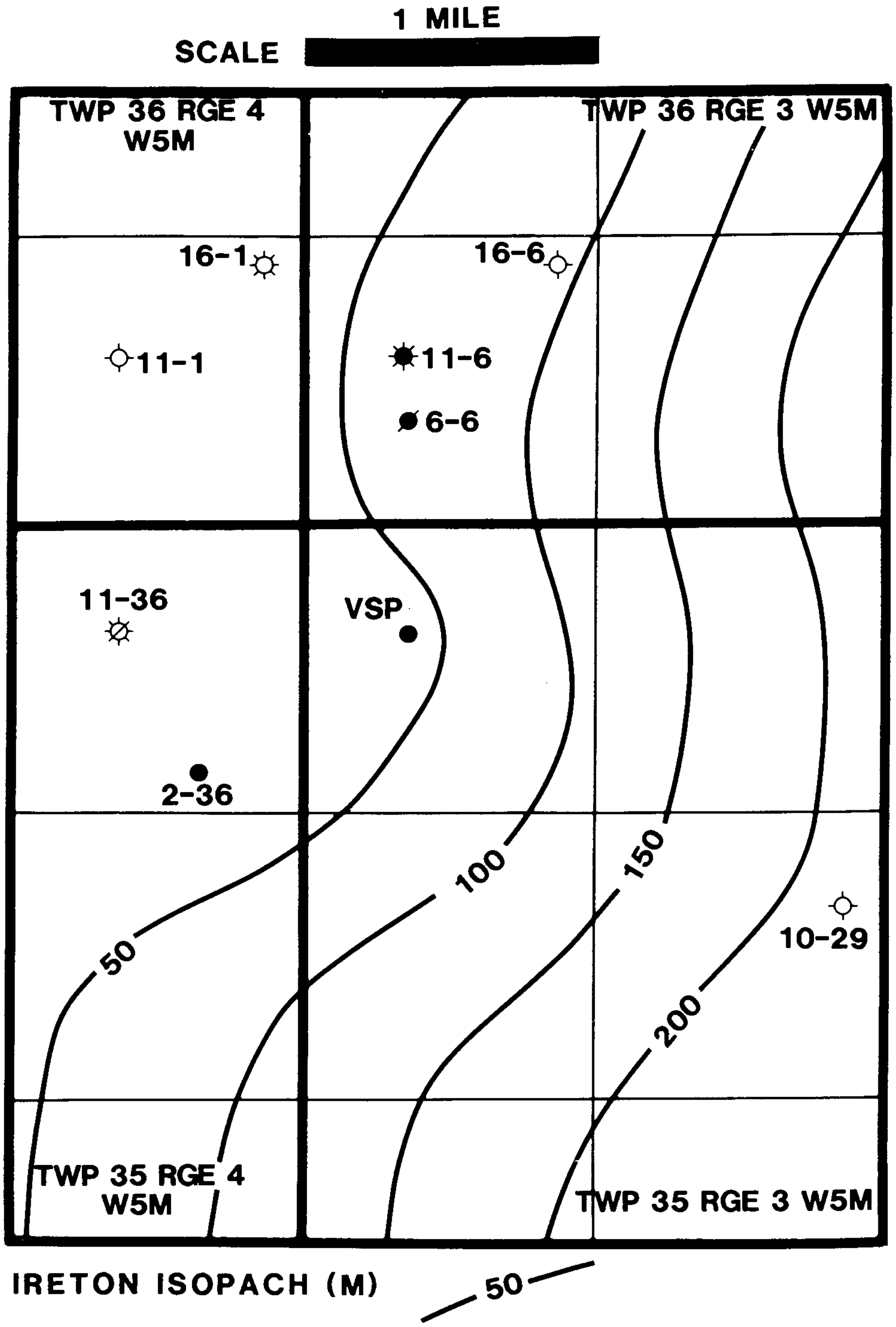

Figure 3.17 Ireton isopach map showing the drape of the Ireton shales along the example seismic line (shown in Figs. 3.14 and 3.15). Considerable time-structural relief along the Ireton event can be correlated from the seismic to the isopach map (from Hinds et al., 1994a and c).

LSD 30 is the mile by a mile section of land directly south of the LSD in which the VSP well was drilled and is shown in Figure 3.17. The Nisku to Ireton anomalous isochron values that are evident at the VSP well location return to normal ranges approximately 640 m south of the VSP well along the seismic line (Fig. 3.17). This can be seen at CDP number 200 in Figure 3.7 and corresponds to the location of the intersection of the seismic line and the 100 m Ireton isopach contour in Figure 3.17. The correlation of the seismic anomaly at the Nisku, Ireton and Leduc levels to the Ireton isopach suggests that the increasing Ireton isopach (away from the well both to the North and South) caused an anomalous seismic response to the subtle drape over the reef crest at the VSP well and this tuning effect can be contributing to the seismic event anomaly (drape and pullup) at the VSP well.

The initial interpretation of the seismic events at the VSP well could then be resolved to be caused by a combination of thinning of the Ireton Formation and an increasing porosity thickness of the Nisku Formation. Part of the Nisku Formation material could be productive as indicated by an anomalous velocity character in the sonic logs (possible patch reef carbonates) that begins approximately 10 m below the Nisku top in the VSP well.

Furthermore, from the inside and outside corridor stacks of both the $\mathbf{Z_{up(decon)}(+TT)}$ and the $\mathbf{Z_{up}(+TT)}$ data as displayed in Figures 3.11 and 3.12, it is apparent that there is multiple contamination immediately below the Wabamun event that may cause difficulties with the interpretation of the Wabamun throughout the study area, and at the Nisku level. However, the effect of the multiple at the Nisku level can account for no more than 5 ms of the anomaly and therefore would be a minor factor in possible causes of the seismic anomaly around the VSP-well.

Other interesting observations can be made from the integrated sonic log, VSP corridor stacks and the seismic data in the immediate vicinity of the VSP well. The Glauconitic to Banff sequence and top of the Leduc are poorly resolved on the surface seismic data (relative to the outside corridor stack). One possible explanation is that the surface seismic signatures of events within the Glauconitic to Banff interval may be degraded as a result of multiple (interbed) interference.

The correlation of the data presented in Figure 3.13 has allowed for the confident reinterpretation of the surface seismic data in the vicinity of the VSP well, and further elucidated the possible origin of the observed anomaly. These reinterpreted seismic data are displayed as Figures 3.14 and 3.15. (The anomaly in the immediate vicinity of the VSP well is enlarged in scale and displayed in Fig. 3.15.)

3.7 Discussion on integrated interpretation

The VSP well was drilled into the Leduc reef at Lanaway Field, south-central Alberta, in order to evaluate an anomaly observed on surface seismic data. The pre-well interpretation of these seismic data suggested that the VSP well would encounter up to 80 m of anomalous accretionary reef growth at the Leduc level. However, drilling confirmed that the Leduc at the VSP well was more-or-less regional and indicated that the initial interpretation was inaccurate as the seismic events were a response to something other than anomalous Leduc buildups and corresponding anomalous Ireton thinning. In order to elucidate the discrepancy between the pre-well seismic interpretation and the drilling results, a near-offset VSP was run at the VSP well site.

The interpretively processed VSP data provided invaluable information regarding the seismic anomaly. On the basis of these data, it was possible to:

1) establish that the Leduc event had been miscorrelated on the pre-well seismic interpretation;

2) correctly correlate the Leduc event at the VSP well site; and

3) further elucidate the nature of the observed anomaly at the VSP well site.

On the basis of VSP data and the integrated interpretation, it has been suggested that the observed seismic anomaly at the VSP well is most likely attributable to (Hinds et al., 1994a):

1) velocity and structural drape resulting from anomalous erosional relief at the pre-Cretaceous subcrop, and the effects of associated interbed multiple reflections;

2) localized patch reef development within the Winterburn Group; and

3) tuning resulting from thinning of the Ireton Formation in the vicinity of the VSP-well.

The most likely effects are the Winterburn patch reef and the tuning effect of an Ireton drape.